International Journal of Research in Engineering and Innovation (IJREI)
journal home page: http://www.ijrei.com
ISSN (Online): 2456-6934

RESEARCH PAPER

Energy-exergy analysis of solar assisted some trigeneration Systems

Radhey Shyam Mishra, Aftab Anjum

Department, of Mechanical and Production Engineering, Delhi Technological University Delhi, India

Article Information

Received: 24 January 2025
Revised: 19 April 2025
Accepted: 10 May 2025
Available online: 14 May 2025

Keywords:

Thermal energy storage
Energy-exergy analysis
Trigeneration Systems
vapor compression-absorption refrigeration system

Abstract

Thermodynamic analysis to analyze thermal performances of combined power and cooling cycle using solar energy as heat source without using thermal energy storage, which provides power and cooling on sunshine hour only and solar driven combined power and cooling cycle with thermal energy storage (TES) is not available in the literature. The helium Brayton cycle has a few points of interest such as simplicity, compactness, superior economy, sustainability, small capital cost because of little size of equipment and plant footprint, improved safety, and high cycle efficiency, in this manner, it is an appealing alternative for power production plants. In this paper, thermodynamic analysis of combined power cycle using ejector-compression cascaded refrigeration system and combined power cycle using vapor absorption refrigeration system combined with heating process. Also, the energy-exergy analysis of combined power and absorption-compression cascaded refrigeration system and combined power, cooling and heating system driven by low temperature heat source using various alternative refrigerants have been presented in this paper.

1. Introduction

Energy is the key to the sustainability of human existence. It is also the measure of prosperity and development in a society. Furthermore, around 80% of the current global energy consumption is fossil fuel-based despite the substantial progress over the last few decades in the field of renewable energy. As a result, the pollution caused due to the burning of fossil fuels, especially the emission of greenhouse gases like CO_2, has led to many environmental issues, such as global warming and climate change. Besides, conventional power plants are relatively inefficient and, could convert only about 30%-35% of the fuel's available energy into power and, a large portion of the remaining energy is rejected to the ambient in the form of low-grade heat that eventually adds up to thermal pollution. In this regard, the use of cutting-edge technologies to reduce global warming and improve the efficiency of energy systems is a crucial goal; Trigeneration systems are one such option that has the potential to meet growing energy demands in a cleaner and more cost-effective manner. Trigeneration systems employ the waste heat recovery principle to simultaneously generate electricity, heating, and cooling from the same fuel source. Particularly, the gas turbine-based trigeneration system finds ample industrial applications, mostly in the process industries, due to its high efficiency, low pollution levels, low capital cost, wide flexibility, and multigenerational capability [1].

The thermal energy that is released into the environment by a process or equipment but which could otherwise be utilized profitably is termed waste heat. Waste heat cannot be avoided because to comply with the second law of thermodynamics, some thermal energy must be released into the environment when heat is transformed into mechanical work. Therefore, it can be inferred that a sizeable amount of fuel energy is lost to the environment and turns into a potential source of thermal pollution. However, both the cost of fuel and environmental damage can be reduced if part of the wasted energy is retrieved employing waste heat recovery systems.

Corresponding author: R. S. Mishra
Email Address: rsmishra@dtu.ac.in
https://doi.org/10.36037/IJREI.2025.9301

1.1 Integrated energy systems

The flue gas from traditional power plants carries away over 61% of the thermal energy, resulting in massive energy and monetary waste. An energy flow diagram for a conventional power plant in which. a significant quantity of fuel energy is lost to the environment. Therefore, it is necessary to further recover the waste heat that was released to increase the fuel conversion potential of a conventional power plant. One of the most effective waste heat recovery strategies is the integration of thermodynamic cycles into the prime mover.

1.2 Cogeneration systems

The cogeneration system, commonly known as the combined heat and power (CHP) system, is the most basic layout of integrated energy systems. The overall thermal efficiency of a system is typically 40-50%, as the fraction of the fuel that is transformed into electricity and heat.
The exhaust gas from the prime mover is typically used to produce either steam using a heat recovery steam generator (HRSG) or hot water using a heat exchanger. A typical layout of a CHP system is shown in Fig. 2.

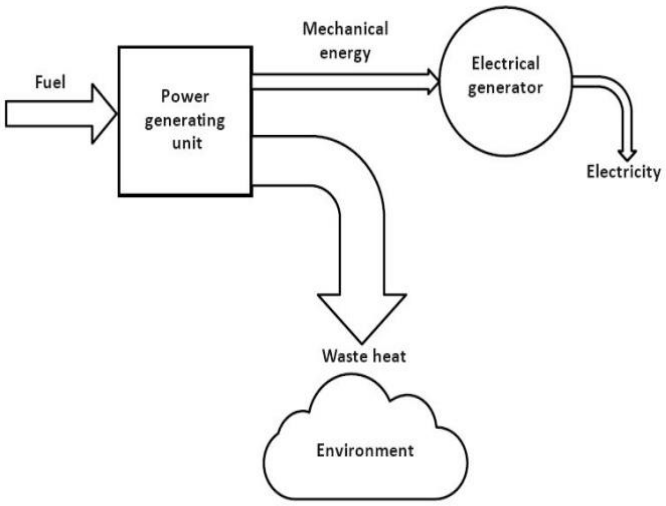

Figure 1: Energy flow diagram for a conventional power plant [6]

1.3 Trigeneration systems

Trigeneration systems simultaneously generate power, cooling, and heating from the same source of fuel. They are the upgraded versions of CHP systems in which some portion of the steam is used to operate the cooling systems while the remaining is used for process heating. They are also known as combined cooling, heating, and power (CCHP) systems [18]. An energy flow diagram for a typical CCHP system is shown in Fig. 3. There are various advantages of a CCHP system which are listed in detail below:

- Improvement in overall efficiency
- Reduction in fuel cost and greenhouse gas emission
- Reduction in greenhouse gas emission
- Cooling system size reduced
- Reduction of capital cost
- Scope of additional revenue generation

A synergetic approach based on the principles of energy analysis, exergy analysis, and environmental analysis [19] can be used to design and develop a thermal system that is efficient and has a low environmental impact. The objective/ contribution in the analysis of a thermal system are as follows [2]:

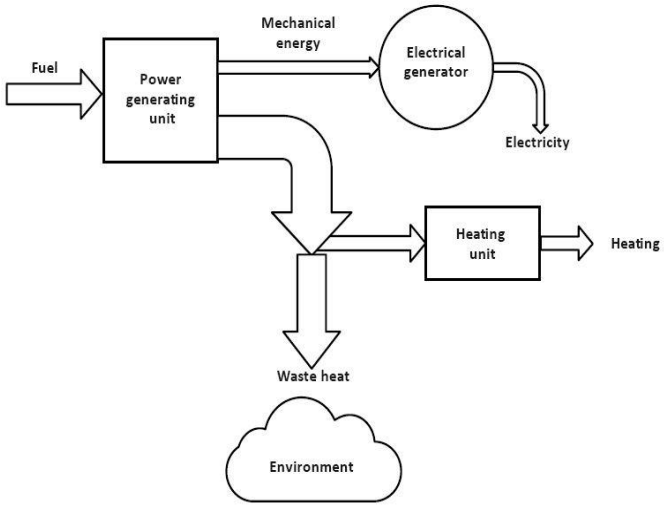

Figure 2: Energy flow diagram for a typical CHP system [6]

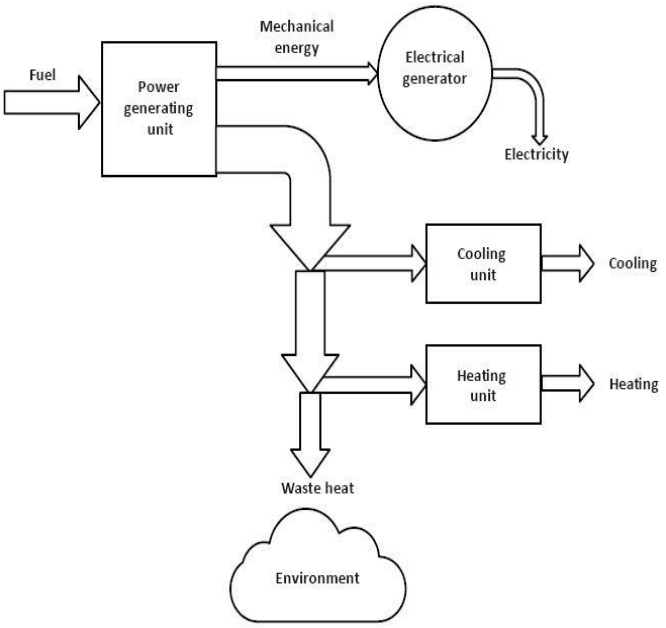

Figure 3: Energy flow diagram for a CCHP system [6]

- Determine the heat and work interactions at each component of a thermal system.
- Identify the source, magnitude, and location of exergy destruction and losses in a thermal system.

- Estimate the environmental impact of pollution emitted by thermal systems.

Based on the above-mentioned literature gaps, the proposed research has been carried out with key objective as "Energy and exergy analyses of four different combined power and cooling systems integrated with an external renewable heat source.

2. Literature review

2.1 sCO2 cycle in trigeneration system (CCHP)

Few investigators have discussed that sCO_2 Rankine cycle has a simplicity and compact structure, and also it can achieve the high efficiency when it was utilized for WHR from a gas turbine as compared to steam/water cycle. They stated that the net output power from a specified source of waste heat can be maximized by incorporating the waste heat utilization efficiency in conjunction with the thermal efficiency of cycle [21]. A comparative analysis was performed on 12 different sCO_2 cycle configurations such as simple recuperated cycle, single heated cascade cycle, recompression, partial heating, pre-compression, dual cascade cycle, single heated cascade cycle with intercooler, intercooled dual heated cascade cycle, dual heated and flow split cycles for triple heating cycle, dual expansion cycle and partial recuperation cycle as land filling gas turbine bottoming. They found various results one the conclusion obtained from their results was that pre-compression and recompression cycle had high thermal efficiency than other considered cycles. They also suggested for future research on combination of both two cycle [22]. The thermodynamic performance and economic analysis of power plant integrated with sCO_2 Brayton power cycle were performed. Finally, their results concluded that as compared to SRC system applied to the exiting coal-fired power plant, SCO_2 power cycle coupled with coal-fired power plant showed an improvement in power generation efficiency of 6.2%-7.4% and levelized cost of electricity was reduced by about 7.8%-13.6% [23]. Experimental investigation was carried out and compared the functioning of trans-critical CO2 (tCO_2) power cycle and R245fa based ORC for low-grade heat power generations. In addition, for these power generation configurations, they utilized the exhaust flue gases from the 80 kWe micro-turbine CHP unit as a heat source. Also, they analyzed the effect of important operational constraints mass flow rate and heat source input etc [24]. The design, cost, and performance of the various configurations of sCO_2 cycle was examined. They found that recompression cycle can attain higher thermal efficiency and partial cooling cycle because of its necessity of higher turbo-machinery capacity, it is the costliest cycle. At last, they reveal that the partial cooling cycle operated by the power tower produces more net electricity and also an inexpensive option [25]. The combined super-critical carbon dioxide (sCO_2) and transcritical carbon dioxide (tCO_2) cycle as a bottoming cycle is proposed. Further multi-objective optimization was performed on the part load condition. They concluded that when the temperature variation of the heat sink was 5–25 °C, the combined sCO_2-tCO_2 cycle could operate within 10–100% of the normalized generator and the corresponding exergetic efficiency of the combined sCO_2-tCO_2 cycle ranged from 24.5 % to 65.7 % [26]. Detailed analysis of the supercritical carbon dioxide recompression Brayton cycle and the tCO_2 cycle as a bottoming cycle assisted with concentrated solar power (CSP) cycle was performed. They found that the efficiency of the combined cycle was enhanced by the use of waste heat and reduced the flow of cooling water. In SPT system they used molten salt for driving the sCO_2recompression cycle. They concluded that sCO_2 cycle is useful for the high temperature application also [27]. Four configurations of the sCO_2 cycles such as precompression, simple recuperated, recompression cycle, and split flow recompression cycle, for recovering the waste heat from the internal combustion exhaust was considered. Further, exhaust heat recovery ratio and thermal efficiency of the four systems were calculated. It was found that the maximum exhaust heat recovery ratio for pre-compression and recuperation of the sCO_2 cycle were achieved at 5.8 MPa and 7.65 MPa, respectively [28].

2.2 ORC system for power generation in CCHP system

The performance and economics of an organic Rankine cycle plant depends on the working fluid used [29]. This justifies the literature dedicated to fluids selection for different heat recovery applications from which properties of good fluids can be summarized [30-35]:

- Vapor saturation curve with zero or positive slope
- High latent heat of vaporization
- High density
- High specific heat
- More critical parameters (temperature, pressure)
- Low viscosity,
- High thermal conductivity
- Stable at high temperature
- Noncorrosive
- High energetic/exergetic efficiency
- Nontoxic and nonflammable
- Low ODP, low GWP
- Low cost and good availability

A solar integrated combined cycle study in which ORC and steam Rankine cycle were used as a bottoming cycle for the recovery of waste heat was carried out. The author considered 15 working fluids in the ORC and found that R1234ze (Z) was the best fluid in terms of thermo-economic, environmental and safety considerations. His work introduces a modified integrated solar combined cycle (ISCC) with two bottoming cycles. The first bottoming cycle is a steam Rankine cycle while the second one is an organic Rankine Cycle ORC [36]. The selection of best working fluid depends on heat source and heat sink profile is carried out. They also mentioned that performance of pure fluids can be better than

mixtures when inlet temperature of heat source will be high and temperature gradient will be low. Furthermore, their study illustrates that the mixtures perform better when inlet temperature of heat source becomes lower, as a result, temperature gradient of both heat source and heat sink become higher. Moreover, they found that heat sources with small temperature gradients require fluids with high critical temperatures and heat sources with large temperature gradients [37]. A 250-kW ORC system with the support of working fluid, for instance R245fa and a turbine expander was examined, and it was reported that the average net power output of 242.5 kW and system thermal efficiency of 8.3% at evaporation temperature of 104.4°C and condensation temperature of 32.3°C. They also noticed that the fluctuation in the net power output was ±1.7 kW, and their results found an improvement in stability of system and developed the system's high potential for on-site WHR applications [38]. The performance of the basic ORC and parallel double evaporator organic Rankine cycle (PDORC) was compared. The applications of zeotropic mixtures and multi-evaporator systems are two viable options to improve the performance ORC. They also conducted economic comparison of a basic ORC with R245fa/R600a and PDORC with R245fa. Four indicators are used to evaluate the system performance: net power, cycle efficiency, area of heat exchangers, and area of heat exchangers per net power output. Sub models of condensers and evaporators are established for pure organic fluids and zeotropic mixtures. The performance optimization using genetic algorithm is conducted to compare the two systems quantitatively [39]. For the energy recuperation from the waste heat rejected by the internal combustion engines, the ORC system is a promising technology stated. They proposed ORC system with dual loop which was made up of two cascaded ORCs that helps in energy recovery from the coolant and exhaust gases of engine, the energy recovery's overall efficiency could be improved. Their study examines the R1233zd and R1234yf based regenerative dual loop ORC system to recover energy from compressed natural gas engine's waste heat [40]. Exergy and energy analysis of supercritical organic Rankine cycle integrated with parabolic trough solar collector (PTSC) is presented with proposed working fluids are R600a, Toluene, R152a, isobutene, and cyclohexane for the supercritical ORC. Performance parameters including exergy efficiency, rate of exergy destruction, improvement potential, fuel depletion ratio, irreversibility ratio and expansion ratio were also examined in this study. The results of the study demonstrate that exergy efficiency increases continuously a both the solar irradiation intensity and inlet pressure of turbine increases, and R600a gives the maximum exergy efficiency among the others [41]. For application of the ORC as bottoming cycle to the exhaust waste heat recovery from diesel engines were reviewed. They found that ORC can achieve up to 25% thermal efficiency, while combined system with diesel engine achieved up to 90% thermal efficiency. Diesel engines play an important role in transport, small medium-size stationary generator, agriculture, as well as generate the biggest CO_2 emission and environmental pollution. However, in fact, more than 60% of energy from air-fuel mixture combustion is not used to produce the mechanical work and is released into the environment as waste heat [42]. Optimization analysis as well as the comparison of single and dual pressure evaporation ORCs were performed. They found that the work output by dual pressure evaporation ORC was more than the single pressure evaporation ORC. Furthermore, as heat source temperature decreased maximum work output increased, and the maximum increments are 21.4–26.7% for nine working fluids [43]. Energetic, exergetic, & financial performance of a solar driven trigeneration system was investigates. They stated that PTSC combined to a storage tank can be used so as to feed an ORC which discards heat to an absorption heat pump. They also optimized the system performance based on the exergy and energy method. Moreover, their results reveal that the heating, cooling, and electricity production were found to be as 995 kWh, 232 kWh and 154 kWh, respectively. At last, they found 5.33 years' payback period and internal return rate of 20.02% that shows a feasible system [44]. A study on the solar energy (i.e. PTSC) and waste heat (i.e. temperature varies from 150℃-300℃) driven hybrid ORC was carried out. They selected four different fluids such as toluene, cyclohexane, MDM, and n-pentane. Their results disclosed that toluene has the ability of highest electricity production, i.e. ranges from 479 kW to 845 kW followed by cyclohexane, MDM and n-pentane [45]. The SORC to recover waste heat at low temperature the recovery of low-grade waste heat was analyzed. They concluded that SORC is an appropriate method for the industrial waste heat recovery and the R152a was observed as the best-performing fluid and produced the maximum net power and thermal efficiency [46]. A parametric analysis of the SORC system for the medium-temperature geothermal heat source was conducted. They concluded that for low-temperature heat sources SORC is more efficient than ORC [47]. A thermal analysis of the SORC and found that SORC has achieved more thermal efficiency and power output than the basic ORC with preheater was conducted [48].

2.3 Recent studies on the ORC-VCC and VAR cycle

A model of the low temperature heat activated combined ORC-VCC system is proposed. They concluded that the computed thermal and electrical COP of the ORC-VCC system varied between 0.30 to 1.10 and 15 to 110 respectively. Additionally, HFO-1234ze (E) was considered an acceptable working fluid for enhanced efficiencies [49]. There is maximum exergy loss in the reactor and there is minimal exergy loss in the components of the VAR cycle. Finally, their results of exergo-economic optimization indicate that the combined configuration has 26.12% and 2.73% greater first and second law efficiency compared to the simple recompression sCO_2 cycle, respectively [50]. The exergy and energy analysis of the ORC integrated VCC system is performed. He concluded that R602 was an acceptable working fluid for system performance and

environmental considerations. Finally, he concluded that the system's highest COP, exergy efficiency, pressure ratio of turbine and the corresponding total mass flow rate of working fluid using R602 were 0.99, 53.8%, 12.2, and 0.005 kg/s -kW respectively at 25°C temperature of condenser [51]. A comparative analysis focused on optimization methods, i.e. single and multi-objective, between the combined sCO_2/lithium bromide-water method and sCO_2/ammonia-water was performed. Their findings show that the sCO_2/ lithium bromide-water device shows a refrigeration COP gain of 0.3112 compared to sCO_2/ammonia-water vapor [52]. The exergy and energy analysis on the combined ORC and single and double evaporator VCC system was performed. They found that R600a was considered as the best fluid for the combined system. They also found that the combined cycle's COP and exergy efficiency with a single evaporator were more than that of a dual evaporator [53]. Thermal and exergo-economic analyzes on the regenerative ORC-VCC system was performed. Their results indicated that among other selected working fluids, the R134a showed the lowest exergy and thermal efficiencies while R143a and R22 showed the highest exergy and energy efficiency respectively. They also observed that the total cost of unit of the product was found to be $60.7/GJ. The maximum exergy destruction was found in the boiler followed by turbine [54].

2.4 Combined cycles

The exergo-economic and comparative analysis of sCO_2/ tCO_2 and sCO_2/ORC configuration was performed and found that at a lower compression pressure ratio, the sCO_2/tCO_2 cycle performs better than sCO_2/ ORC. Moreover, it was found that as compared to sCO_2/tCO_2 cycle, the sCO_2/ORC cycle has slightly lower value of total product unit cost [55]. Novel cogeneration system, which was a grouping of Rankine power cycle & absorption refrigeration cycle for recovery of industrial waste heat in order to produce combined power and refrigeration was proposed. Their results revealed that with upsurge in gas inlet temperature, power to cold ratio increases while first law efficiency decreases. However, with increase in pitch point, exergy efficiency and power to cold ratio decreases while first law efficiency increases [56]. The two cogeneration cycles in which waste heat was recuperated by either TCO_2 cycle or ORC from a R-SCO_2 Brayton cycle in order to generate electricity was examined by selecting the organic fluids such as R123, R245fa, toluene, isobutene, isopentane, and cyclohexane as working fluids [57]. The performance of a combined gas and steam turbine cycle power plant coupled by a ORC and VAR cycle is carried out. by performing energy, exergy, and environment sustainability index analysis and their results reveal that through the R113 based ORC which has been operated by the waste exhaust heat of a combined cycle power plant was generated extra 7.5 MW of electricity and additional 51.1 MW electricity was produced with the utilization of VAR cycle so as to cool inlet air stream to 15℃ in the gas turbine plants [58]. An energy and energy analysis on the model of integrated solar parabolic trough collectors, combined with the simple recuperated sCO_2 cycle and the ORC as a bottoming cycle was carried out and concluded that the system's exergetic and energetic efficiency increased with solar irradiation, and the fuel depletion ratio and the highest power output were found to be 0.2583 and 3740 kW respectively at 0.85kW/m^2 of solar irradiation [59].

2.5 Review on refrigeration systems

The refrigeration has many applications in human life for cooling and air-conditioning, fruits, vegetables, pharmaceutical products conservation and maintaining environmental conditions etc. For the design and growth of solar energy conversion systems like ejector refrigeration, a detailed knowledge of available solar radiation is required. The use of the solar energy as the heat source for ejector refrigeration and absorption refrigeration system has studies by the many researchers. The ejector is the heart of the ejector cooling system, which increases the pressure without consuming mechanical energy directly. Due to this the ejector is a simple and safer device than a compressor or a pump which can increase pressure. The basic principle of the ejector cycle based on gas dynamics was introduced [60], and then developed [61, 62]. Solar absorption system using LiBr-H_2O was being simulated and correlation has been drawn between hot water inlet temperature, COP and surface area of absorption through their findings. The finding that shows that the total exergy destruction is greater in NH3-H_2O than LiBr-H_2O has been examined [63]. The major contributor of the exergy destruction has been found to occur in generator and absorber and it is also stated that increase in temperature of the absorber can actually contribute in increasing the exergetic efficiency. The energy and exergy analyses of a single effect lithium bromide absorption refrigeration system carried out. They observed that COP and exergy efficiency increases with the increase in generator temperature (750°C to 1100°C) and the maximum exergy destruction occurs in the generator & followed by the absorber [64]. The thermodynamic analysis of a new combined cooling and power system using ammonia–water mixture by using low grade heat sources is carried out. Exergy destruction study was conducted to identify the exergy distribution in the various components. The result shows that the major exergy destruction takes place in the heat exchangers [65]. A computer program for a combined power and ejector cooling cycle using R123 as the working fluid to determine the effects of various operating parameters on the performance of the cycle have been done and numerical computation was carried out. Their results show that the first and second law efficiency increase with the increase in evaporator temperature, and maximum exergy losses occurs in the boiler and ejectors. In addition to this, there is increase in first law efficiency and decrease in second law efficiency with increase in turbine inlet pressure [66-72]. The recent studied on trigeneration systems were given in Table 1.

Table 1: Recent studies on trigeneration Systems

Year	Brief title	Methods adopted	Working fluid used	Major observations	Ref.
2015	Multi-objective optimization of a combined cooling, heating and power system driven by solar energy	The multi-objective optimization and mathematical modeling was carried out.	R245fa and water	Turbine inlet temperature, turbine inlet pressure, condensation temperature and pinch temperature difference in vapor generator, were selected as the decision variables to examine the performance of the overall system.	73
2016	Analysis of a novel combined power and ejector-refrigeration cycle	Parametric analysis of the combined cycle has been carried out	zeotropic mixture, isobutane/pentane	The cycle exergy achieves a maximum value of 10.29% with mixture isobutane/pentane (40%/60%), and the thermal efficiency gets a maximum value of 10.77% with mixture isobutane/pentane (70%/30%).	74
2016	Energy and exergy analysis of a closed Brayton cycle based combined cycle for SPT plant.	Energy and exergy analysis was done	helium	The exergy efficiencies of higher than 30% are achieved for the overall power plant. The power cycle has a better performance than the other investigated Rankine and supercritical CO_2 systems.	75
2017	Investigation on the combined Rankine-absorption power and refrigeration cycle	Parametric analysis and genetic algorithm has been adopted	liquid mixture of water and ammonia	Environmental temperature, heat source, refrigeration, inlet pressure, and temperature, and the density of the ammonia-water dilution have major effects on the exergy efficiency, the refrigeration output, and the net power of the system.	76
2017	waste heat based organic Rankine cycle powered cascaded vapor compression-absorption refrigeration system	Energy and exergy calculations used through various equations used	dry organic working fluid	The energetic efficiency of the present system for only cooling mode and cogeneration mode (cooling and heating) are calculated to be 22.3% and 79%, respectively.	77
2020	performance comparison of various solar-driven novel combined cooling, heating and power system topologies	Theoretical analysis and the thermodynamic (energy and exergy) was performed	natural (eco-friendly) substance, n-butane	The objective functions like performance index, irreversibility, exergy efficiency, net work output, heating output, entrainment ratio and cooling output was analyzed on the basis of generator temperature, evaporator temperature, condenser temperature and solar intensity.	78
2020	A novel integrated solar gas turbine trigeneration system for production of power, heat and cooling	Economic-thermodynamics-environmental analysis of the system has been carried out.	Chilled water and steam	The hourly and yearly performance of the considered plants with different gas turbine and solar field sizes have been examined and most proper location to utilize the solar hybrid power plants is in locations with high levels of solar irradiance and low ambient temperature.	79
2021	combined solar based pre-compression supercritical CO_2 cycle and organic Rankine cycle using ultra low GWP fluids	Parametric thermodynamic and economic analysis has been carried out	HFO (hydro fluoro olefins) and R134a	It was observed that HFO performed better than the R134a. R1336mzz (Z) gave highest thermal and exergy efficiency and power output for the combined cycle by 55.02, 59.60%, 298.5 kW at 950 W/m^2 of solar irradiation respectively.	80
2021	Performance evaluation of solar based combined pre-compression supercritical CO_2 cycle and ORC	Parametric thermal modeling has been carried out	R227ea	Net power output and thermal efficiency of pre-compression cycle was improved by 4.51 and 4.52%, respectively, using ORC. Highest thermal, exergy efficiency, and power output increased with irradiation.	81
2022	Assessment of a novel solar-based trigeneration system; investigation of zeotropic mixtures.	energy and exergy analysis in MATLAB software	zeotropic mixtures	The electrical power, cooling load, and heating capacity were calculated and the highest exergy and energy efficiencies were computed by 20.26% and 15.81%, respectively.	82
2023	Recent progress in thermal and optical enhancement of low temperature solar collector	Various technical progress in thermal and optics are studied	nano-fuids	The most important parameters affecting the solar collector's performance is the geometry of the solar collectors, also it can conclude that design of solar collectors can reduce their costs by 10%.	83
2023	Study of combined cycles for concentrated solar power for power generation using low GWPfluids to reduce environmental effects	Parametric analysis and mathematical modeling was done	R1243zf, R1234ze€ R1224yd(Z), R1336mzz(Z)	This configuration's highest thermal and exergy efficiencies were discovered to be 51.9% and 55.84%, respectively, and R1243zf was found to be the best-performing fluid among other considered low GWP fluids to reduce the environmental effects.	84

2023	Investigation of new combined cooling, heating and power system based on solar thermal power and single-double-effect refrigeration cycle	System energetic an d ex rgetic modeling has been carried out	CO_2	The influence of variation in temperature of pump entry and evaporator chiller on generation of power, refrigeration effect, co oling exergy, efficiencies of CCHP is analyzed. Resul ts yield a first law efficiency between 64-72%, and second law efficiency from 19% to 25% wit h the rise of solar irradiation from 400 to 1000 W/m^2.	85
2023	Exergoeconomic and thermodynamic analyses of solar power tower based novel combined HBC-tCO_2 cycle for carbon free power generation	exergoeconomic and thermodynamic analyses was done	CO_2, helium	The exergy and thermal efficiency of the SPT-based combined cycle are enhanced by 13.18% and 13.21% respectively, while electricity cost is reduced by around 2% as compared to the SPT-based basic cycle (SPT-HBC) configuration at base conditions.	86
2023	Parametric analysis and optimization of a novel cascade compression-absorption refrigeration system integrated with a flash tank and a reheater	The energy and exer gy method, parametr ic analysis, and opti mization by genetic algorithm for two di fferent refrigerant pa irs.	R41, lithium bromi de solution (L iBr/H_2O) and ammonia solu tion (NH_3/H_2 O)	At an evaporator temperature of −35 °C, the proposed system is capable to achieve 15.39% higher COP and exergetic efficiency and employing R41-NH_3/H_2O combination under identical working condit ions, the proposed system has achieved 18.49% highe r COP and exergy efficiency than the conventional ca scade absorption cycle.	87
2023	Investigation of an ejector-cascaded vapor compression–absorption refrigeration cycle powered by linear Fresnel and ORC	A thermodynamic and thermo-economic analysis w as performed,	Toluene, R1234yf, LiBr/H_2O	Based on the results, the energy and exergy efficienci es vary from 38 to 50% and from 3.6 to 4.6%, respecti vely. The cascade cycle COP and the system overall efficie ncy improvement were obtained as 27.02% and 51.19 %% over the cycle without ejector.	88
2023	investigation and multi-objective optimization of a novel efficient solar tower power plant based on supercritical Brayton cycle with inlet cooling	The energy and exer gy method, parametr ic analysis has been carried out.	helium	HBC is employed as the topping Cycle and the vapor absorption cycle are used as the bottoming cycle. They conclude that optimized combined cycle's energy efficiency is 14.5% higher than that of the basic cycle. Helium performs better than sCO_2 at high turbine input temperatures.	89
2024	Development and assessment of a novel multi-generation plant combined with a supercritical CO_2 cycle for multiple products	Thermodynamic assessment is conducted with energy and exergy analysis	CO_2	The net power, hydrogen, and freshwater production capacities of the reference study are calculated to be 1336 kW, 0.002004 kgs^{-1}, and 0.954 kgs^{-1}, respectively and energetic and exergetic performances are 55.76% and 52.17.	90
2024	Performance comparison of organic Rankine cycles integrated with solar based combined cycle	An exergo-environmental analysis performed	CO_2	It was concluded that the addition of basic ORC and PDORC to the standalone intercooled cascade sCO_2 cycle enhanced the thermal efficiency by 2.26% and 6.66% respectively at 950W/m^2 of direct normal irradiation.	91

A lot of researchers focused their work on combined power and vapor absorption refrigeration cycle, but very few concentrate their work on the combination of organic Rankine cycle and ejector refrigeration cycle. Most of the research work has been done for the performance estimation of the combined power, heating and ejector cooling cycle based on the 1st law of thermodynamics but very few concentrate on the 2nd law of thermodynamics for performance estimation. It has been found that very limited studies are available with regard to the performance evaluation of SPT driven combined cycle especially in which HBC cycle is acting a topping configuration and ORC as a bottoming cycle and can further improved by utilizing waste heat [81, 89]. In the literature, exergy and energy analysis of PTSC integrated combined simple sCO_2 cycle-ORC and recompression sCO_2 cycle-ORC were performed. However, there are various configurations of the HBC cycles with utilizing the waste heat, whose performance need to be investigated when driven SPT and combined with bottoming ORC-ERS system. Also, performance of these systems needs to be compared with previous studies [86]. Apart from sCO2 cycles, also a parametric analysis of the SPT integrated combined SORC and VAR/VCC need to be discussed for combined cooling, heating and power generation. It is clear from the literature mentioned above that not many studies were done on Brayton cycle using helium as the working fluids also no study was performed for low temperature cooling using high temperature solar heat from SPT system. Additionally, the ORC was utilized in the majority of earlier studies as the bottoming cycle [80, 85]. To fulfill this research gap cascaded VAR-VCR system is used as bottoming cycle for recovering the waste heat from the toping cycle for heating application and cooling at low temperature for food preservation etc. utilizing the solar heat from the high temperature SPT system need to be investigated [77,79]. Research work has been done to analyze the combined power and cooling cycle using solar

energy as heat source without using thermal energy storage (TES), which provides power and cooling on sunshine hour only. But the research contribution on solar driven combined power and cooling cycle with thermal energy storage (TES) is not available in the literature. The helium Brayton cycle has a few points of interest such as simplicity, compactness, superior economy, sustainability, small capital cost because of little size of equipment and plant footprint, improved safety, and high cycle efficiency, in this manner, it is an appealing alternative for power production plants. In this paper, thermodynamic analysis of combined power cycle using ejector-compression cascaded refrigeration system and combined power cycle using vapor absorption refrigeration system combined with heating process. Also the thermal analysis of combined power and absorption-compression cascaded refrigeration system and combined power, cooling and heating system driven by low temperature heat source using various alternative refrigerants.

3. System description

3.1 Solar based novel tri-generation system for combined cooling, heating and power generation

In the current study, a novel trigeneration system was to utilize the solar energy from the solar power tower for combined heating cooling and power generation is shown in Fig-4. The trigeneration system consist a Brayton cycle in which helium was considered as working fluid and organic Rankine cycle (ORC) with ejector refrigeration system (ERS) was used for recovering the wasted heat from the Brayton cycle. The power was produced by the Brayton cycle and ORC whereas, cooling and heating was produced simultaneously by the condenser and evaporator respectively. For building applications such as hospitals and hostels, the heating and cooling effects were generated at 50°C and 10°C respectively. Finally, the optimal system exhibits exergy and energy efficiency of 25.12% and 23.3%, respectively, when all the studied parameters are taken into consideration. Apart from this power output, heating and cooling productions were 14998 kW, 60.52 kW and 8.25 kW and respectively at the 2.3 of compressor pressure ratio, 197.2°C of inlet temperature of ORC turbine and isopentane as working fluid.

3.2 Thermodynamic Energy and exergy analysis

The total system is broken down into the three sub systems solar sub-system and the HBC and ORC, ERS for thermodynamic study (fig-5). Each component in the system is given a thermodynamic model, and the computational software Engineering Equation Solver (EES) is taken to simulate the model. Taking control volume approach the equation for the energy and exergy balance equation following steady state conditions can be written as

$$\dot{Q}_{CV} - \dot{W}_{CV} + \sum(\dot{m}_i h_i) - \sum \dot{m}_e h_e) = 0 \quad (1)$$

$$\dot{E}D = \dot{E}X_{in} - \dot{E}X_{out} \quad (2)$$

$$\dot{E}X_j = \dot{m}\cdot[(h_j - h_0) - T_0(s_j - s_0)] \quad (3)$$

$$\dot{Q}_{rec,in} = \eta_{field}\cdot\dot{Q}_{Sun} = \eta_{field}\cdot DNI \cdot A_{hel} \cdot N_{hel} \quad (4)$$

Where, η_{field} is the heliostat field efficiency (optical), and expressed as;

$$\eta_{field} = \eta_{cos}\cdot \eta_{s\&b} \cdot \eta_{int} \cdot \eta_{att} \cdot \eta_{ref} \quad (5)$$

Where,η_{cos}, $\eta_{s\&b}$, η_{int}, η_{att}, η_{ref} represents the efficiencies of the cosine effect, shading and blocking, interception efficiency, atmospheric attenuation and heliostats reflectivity respectively.

$$\eta_{rec} = \frac{\dot{Q}_{rec,net}}{\dot{Q}_{rec,in}} \quad (6)$$

$$\dot{Q}_{rec,in} = \dot{Q}_{rec,in} + \dot{Q}_{rec,loss} = \dot{m}_{air}(h_{16} - h_{17}) + \dot{Q}_{rec,loss} \quad (7)$$

$$\eta_{en} = \frac{\dot{W}_{net}+\dot{Q}_E+\dot{Q}_C}{\dot{Q}_{Sun}} \quad (8)$$

$$\eta_{ex,} = \frac{\dot{W}_{net}+\dot{Q}_E\cdot\left(1-\frac{T_0}{T_E}\right)+\dot{Q}_C\cdot\left(1-\frac{T_0}{T_C}\right)}{\dot{Q}_{Sun}\cdot\left(1-\frac{T_0}{T_{ref,Sun}}\right)} \quad (9)$$

$$\dot{W}_{net} = \dot{W}_{HT} - \dot{W}_{HC} + \dot{W}_{OT} - \dot{W}_{pump} \quad (10)$$

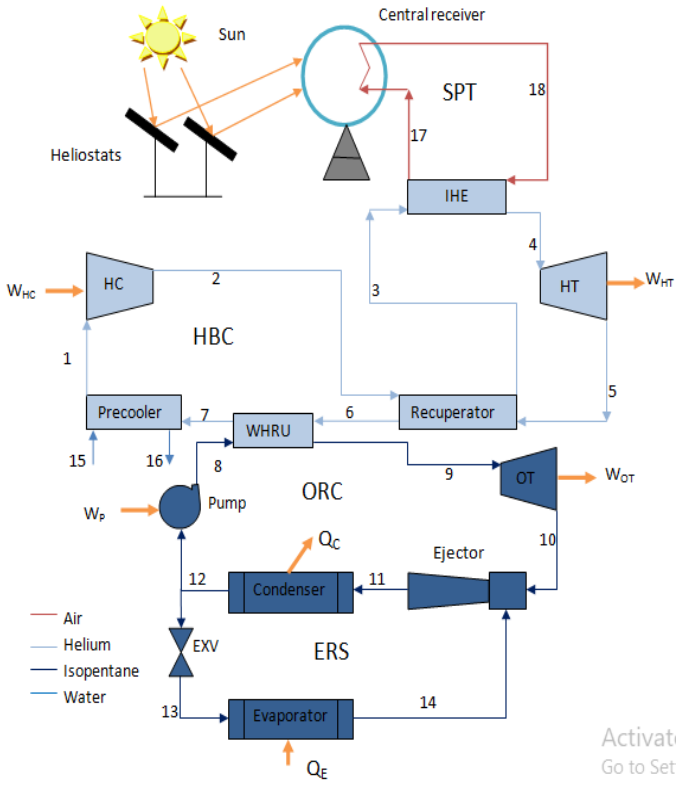

Figure 4: Schematic diagram of proposed trigeneration system integrated SPT plant

It is crucial to note that at the state point (pf1), the inflow velocity is insignificant. The motive nozzle's energy conservation can be expressed as follows:

$$h_{pf1} = h_{pf2} + \frac{V_{pf2}^{\ 2}}{2} \quad (11)$$

Also its nozzle efficiency (η_n) is expressed as:

$$\text{The } \eta_n = \frac{(h_{pf1} - h_{pf2})}{(h_{pf1} - h_{pf2,s})} \quad (12)$$

Suction nozzle

$$h_{sf1} = h_{sf2} + \frac{V_{sf2}^{\ 2}}{2} \quad (13)$$

$$\eta_n = \frac{(h_{sf1} - h_{sf2})}{(h_{sf1} - h_{sf2,s})} \quad (14)$$

The entertainment ratio (μ) is a crucial variable for ejector modelling. The entertainment ratio (μ) is the ratio of the mass flow rate of secondary flow to the primary flow can be expressed as:

$$\mu = \frac{m_{sf}}{m_{sf}} \quad (15)$$

$$V_{pf} + \mu \cdot V_{pf} = (1 + \mu) \cdot V_{mf,s} \quad (16)$$

$$\eta_m = \frac{V_{mf}^{\ 2}}{V_{mf,s}^{\ 2}} \quad (17)$$

$$V_{mf} = \sqrt{\eta_m} \cdot \left(\frac{1}{1+\mu} \cdot V_{pf} + \frac{\mu}{1+\mu} V_{sf}\right) \quad (18)$$

The conversion energy can be written as:

$$(1 + \mu) \cdot \left(h_{mf} + \frac{V_{mf}^{\ 2}}{2}\right) = \left(h_{pf} + \frac{V_{pf}^{\ 2}}{2}\right) \cdot \mu \cdot \left(h_{sf} + \frac{V_{sf}^{\ 2}}{2}\right) \quad (19)$$

d) Diffuser section

$$h_d = h_{mf} + \frac{V_{mf}^{\ 2}}{2} \quad (20)$$

$$\eta_d = \frac{(h_{d,s} - h_{mf})}{(h_d - h_{mf})} \quad (21)$$

3.3 Solar based power cycle integrated compression-absorption cascaded system

This work developed a trigeneration system for SPT plant that produces power, heating and cooling at low temperature efficiently from a high temperature SPT heat source is shown in fig 6. In order to create heating and low temperature (at -20°C) cooling benefits for food preservation, this trigeneration unit integrates a cascaded vapour compression-absorption refrigeration system combined with a helium Brayton cycle for power generation. The exergy-energy analysis was performed by the numerical technique using engineering equation solver software to evaluate the performance of the proposed SPT plant. The power output, exergy and energy efficiency of the SPT plant were found as 14865 kW, 39.53% and 28.82%, respectively. The coefficient of performances values for cooling and heating were observed as 0.5391 and 1.539 respectively. Furthermore, a comparative analysis with relevant previous studies has shown that the proposed system (fig-6) outperforms systems based on supercritical CO_2 cycles and the Rankine cycles.

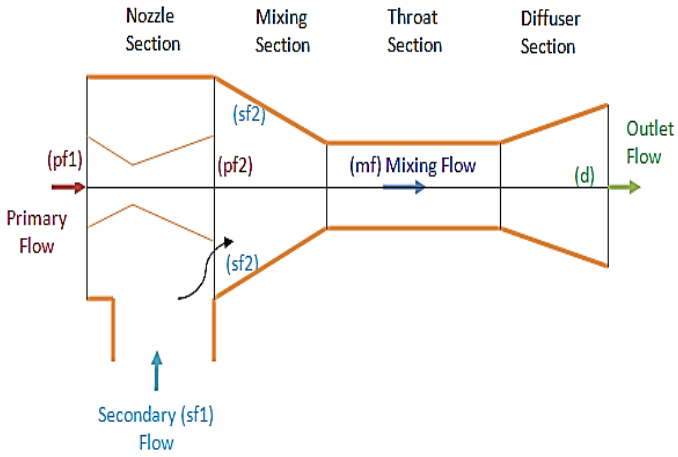

Figure 5: Model of ejector device for the mathematical modeling

3.4 Thermodynamic modeling of proposed cycle

$$\dot{Q}_{CV} - \dot{W}_{CV} + \sum(\dot{m}_i h_i) - \sum(\dot{m}_e h_e) = 0 \quad (22)$$

$$\dot{ED} = \dot{X}_{in} - \dot{X}_{out} \quad (23)$$

The concept of exergy is used to evaluate second-law performance. The four components of total exergy for a fluid stream are as follows [64]:

$$\dot{X}_j = \dot{X}_{ph} + \dot{X}_{ch} + \dot{X}_{ke} + \dot{X}_{pe} \quad (24)$$

$$\dot{X}_j = \dot{X}_{ph} = \dot{m} \cdot [(h_j - h_0) - T_0(s_j - s_0)] \quad (25)$$

The sun irradiation per unit area (DNI) and total area of heliostat field (A_{hel}) determine the total solar heat obtained by the heliostats. The expression for this parameter is:

$$\dot{Q}_{solar} = DNI \cdot A_{hel} \cdot N_{hel} \quad (26)$$

$$\dot{Q}_{rec} = \eta_{field} \cdot \dot{Q}_{solar} \quad (27)$$

$$\eta_{field} = \eta_{cos} \cdot \eta_{s\&b} \cdot \eta_{int} \cdot \eta_{att} \cdot \eta_{ref} \quad (28)$$

$$\eta_{rec} = \frac{\dot{Q}_{rec,net}}{\dot{Q}_{rec,in}} \quad (29)$$

The net heat transfer through the receiver can be defined as;

$$\dot{Q}_{rec,net} = \dot{m}_{air} \cdot (h_{30} - h_{31}) \quad (30)$$

$$\dot{Q}_{rec,net} = \dot{Q}_{rec,in} + \dot{Q}_{rec,loss} \quad (31)$$

$$\eta_{en,plant} = \frac{\dot{W}_{net}+\dot{Q}_e+\dot{Q}_a+\dot{Q}_c}{\dot{Q}_{solar}} \quad (32)$$

$$\eta_{ex,plant} = \frac{\dot{W}_{net}+\dot{X}_e+\dot{X}_a+\dot{X}_c}{\dot{Q}_{solar}\cdot\left(1-\frac{T_0}{T_{Sun}}\right)} \quad (33)$$

$$\dot{W}_{net} = \dot{W}_{HT} - \dot{W}_{HC} - \dot{W}_{Comp} - \dot{W}_{pump} \quad (34)$$

$$\eta_{en,comb} = \frac{\dot{W}_{net}+\dot{Q}_e+\dot{Q}_a+\dot{Q}_c}{\dot{Q}_{IHE}} \quad (35)$$

$$\eta_{ex,comb} = \frac{\dot{W}_{net}+\dot{X}_e+\dot{X}_a+\dot{X}_c}{(\dot{X}_{30}-\dot{X}_{31})} \quad (36)$$

Where, $(\dot{X}_{30} - \dot{X}_{31})$ refers to exergy supplied by the IHE to trigeneration system (HBC-VAR-VCR) [88]

$$COP_h = \frac{\dot{Q}_a+\dot{Q}_c}{\dot{Q}_g+\dot{W}_{Comp}+\dot{W}_P} \quad (37)$$

However, cooling effect is taken by the evaporator only. Therefore, COP for cooling can be evaluated as [74];

$$COP_c = \frac{\dot{Q}_e}{\dot{Q}_g+\dot{W}_{Comp}+\dot{W}_P} \quad (38)$$

The individual COPs of the VAR and VCR can also be defined as the useful output to the input energy to that cycle. COP of the VAR system is calculated as:

$$COP_{VAR} = \frac{\dot{Q}_{cc}}{(\dot{Q}_g+\dot{W}_p)} \quad (39)$$

However, COP of the VCR system is calculated as;

$$COP_{VCR} = \frac{\dot{Q}_e}{\dot{W}_{Comp}} \quad (40)$$

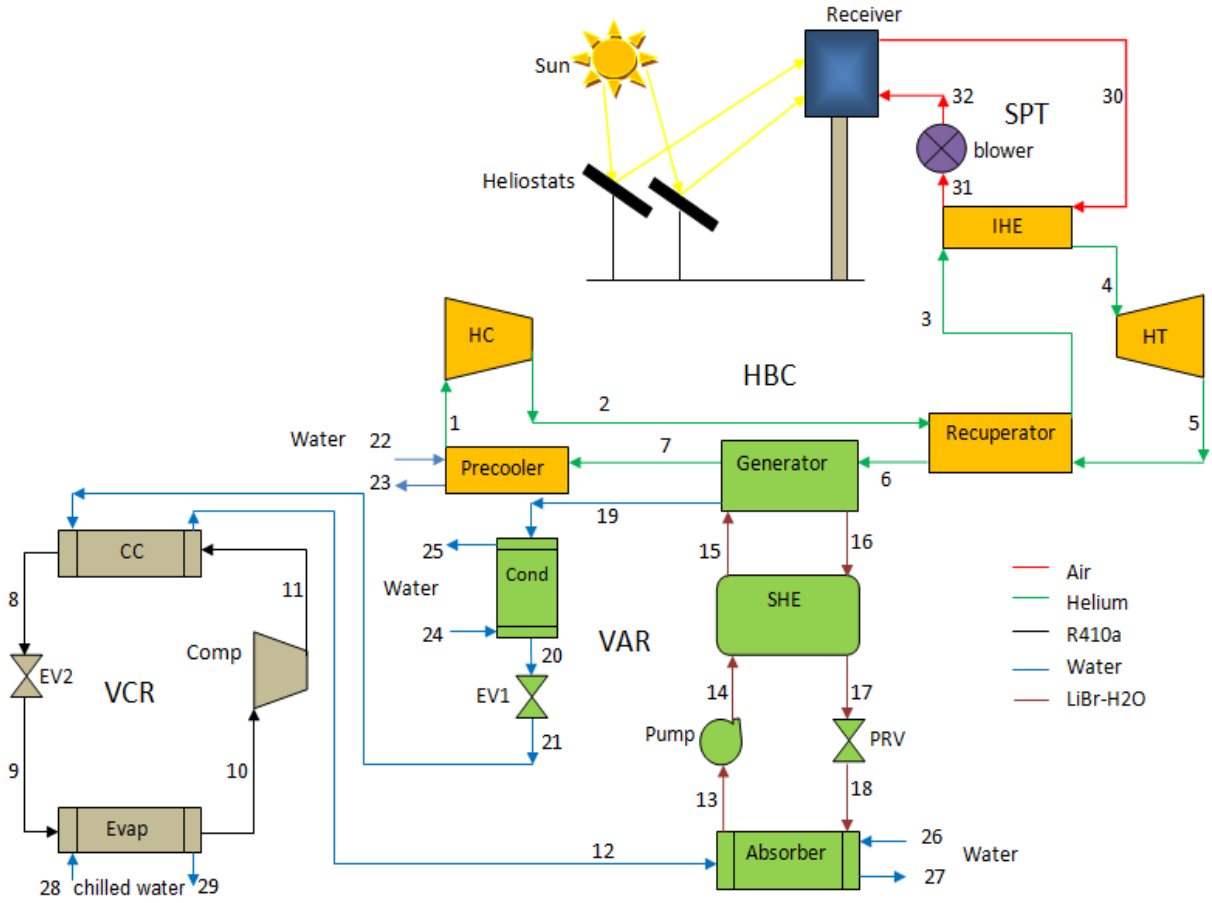

Fig. 6: Schematic diagram of proposed solar based CCHP system

3.5 Solar based power cycle integrated cascaded ejector-vapor compression refrigeration system

In the present work a solar based a novel trigeneration system is proposed to produce the power, heating and cooling at low temperature (-40°C) for food storage application is shown in Fig-7. The organic Rankine (ORC) cycle, cascaded ejector refrigeration system (ERS)-vapor compression refrigeration (VCR) system has been implemented to the solar power tower (SPT) based conventional helium Brayton cycle (HBC) to enhance the performance of the solar based energy generation system. The energy, exergy analysis and

parametric analysis have been carried out using engineering equation solver software. It was concluded that overall proposed solar plant (SPT-HBC-ORC-ERS-VCR) obtained the energy efficiency, exergy efficiency and net work output as 60.66%, 35.55% and 15585 kW respectively. Additionally, heating and cooling effects were obtained as 14967 kW and 730 kW for the industrial application and food storage application respectively. Exergy efficiency of the proposed system is 10.09% higher than conventional plant. Parametric analysis revealed that the solar parameters affected much the performance of the proposed plant.

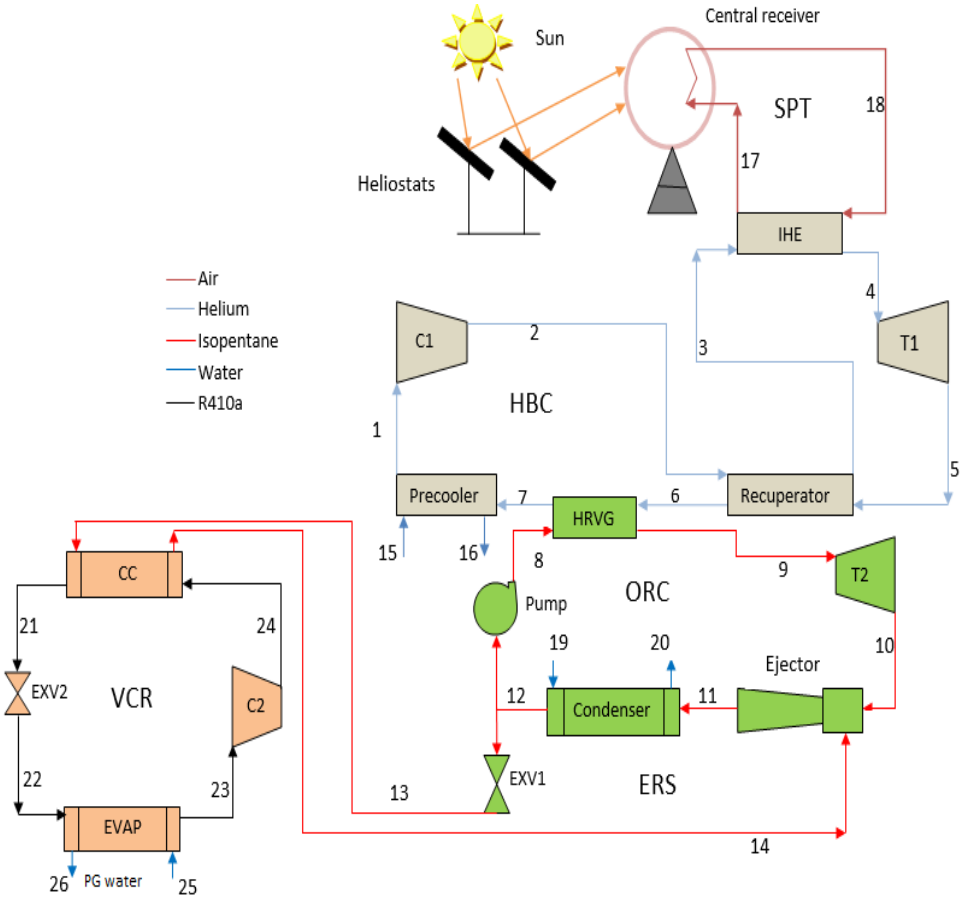

Figure 7: Schematic diagram of the proposed solar based trigeneration system

Thermodynamic modeling of proposed cycle(fig-7) is given below

$$\dot{Q}_{CV} - \dot{W}_{CV} + \sum(\dot{m}_i h_i) - \sum(\dot{m}_e h_e) = 0 \quad (41)$$

$$\dot{ED} = \dot{EX}_{in} - \dot{EX}_{out} \quad (42)$$

$$\dot{EX}_j = \dot{m}\cdot[(h_j - h_0) - T_0(s_j - s_0)] \quad (43)$$

$$\dot{Q}_{rec,in} = \eta_{field}\cdot\dot{Q}_{Sun} = \eta_{field}\cdot DNI \cdot A_{hel} \cdot N_{hel} \quad (44)$$

Where, heliostat field efficiencyη_{field} is expressed as (Zare et al. 2016);

$$\eta_{field} = \eta_{cos}\cdot\eta_{s\&b}\cdot\eta_{int}\cdot\eta_{att}\cdot\eta_{ref} \quad (45)$$

However the receiver efficiency and heat transfer are expressed as (Wang et al. 2011);

$$\eta_{rec} = \frac{\dot{Q}_{rec,net}}{\dot{Q}_{rec,in}} \quad (46)$$

$$\dot{Q}_{rec,in} = \dot{Q}_{rec,net} + \dot{Q}_{rec,loss} = \dot{m}_{air}\cdot(h_{16} - h_{17}) + \dot{Q}_{rec,loss} \quad (47)$$

$$\eta_{en,Plant} = \frac{\dot{W}_{net} + \dot{Q}_{EVAP} + \dot{Q}_{COND}}{\dot{Q}_{Sun}} \quad (48)$$

$$\eta_{ex,Plant} = \frac{\dot{W}_{net,Plant} + \dot{Q}_{EVAP}\cdot\left(1 - \frac{T_0}{T_E}\right) + \dot{Q}_{COND}\cdot\left(1 - \frac{T_0}{T_{COND}}\right)}{\dot{Q}_{Sun}\cdot\left(1 - \frac{T_0}{T_{Sun}}\right)} \quad (49)$$

Where, T_{Sun} is the apparent temperature of the sun used as the exergy assessments (Wang et al. 2011), However, $\dot{W}_{Plant}$ of the plant is expressed as:

$$\dot{W}_{Plant} = \dot{W}_{T1} + \dot{W}_{T2} - \dot{W}_{C1} - \dot{W}_{C2} - \dot{W}_{pump} \quad (50)$$

3.6 Combined Rankine-absorption power and refrigeration cycle with heating process in a tri-generation system

A combined power and refrigeration cycle is proposed, which combines the Rankine absorption refrigeration cycle using binary liquid mixture of water and ammonia as working fluid, produces both power output and refrigeration output simultaneously with only one heat source is shown in Fig-8 . A thermodynamic analysis has been carried out to investigate the key thermodynamic parameters effects on the performance of the combined cycle using engineering Equation solver (EES). It is shown that heat source temperature, ambient temperature, refrigeration temperature, turbine inlet pressure, turbine inlet temperature and basic solution ammonia concentration have significant effects on the net power output, refrigeration output and exergy efficiency of the combined cycle. It is shown that heat exchanger exhaust is the biggest source of exergy destruction followed by the heat exchanger, boiler, turbine, super heater, absorber, condenser and rectifier respectively. Both energy and exergy efficiencies of the integrated system and exergy loss distributions of heat input source are computed and compared with energy distribution. This Combined cycle is ideally suited for solar thermal power using low cost concentrating collectors.

3.7 Combined power, heating and cooling cycle using low temperature heat source with various eco-friendly refrigerants

This study describes an integrated power, cooling, and heating cycle that incorporates an ejector refrigeration system, an ORC and condenser heating with a low temperature heat source. Thermodynamics' first and second laws were used to analyze the performances of six distinct alternative refrigerants on the combined cycle. The influence of the most important parameters including evaporator temperature, turbine entering temperature heat source temperature on the refrigeration output, exergy efficiency, entrainment ratio, thermal efficiency, total exergy destruction and thermal efficiency of the stated system using different environmentally friendly working fluids (R-123, R-124, R-141b, R-290, R-134a, and R-152a) were studied. Out of all the working fluids employed in this study, R-152a and R-134a are the most appropriate from an energy efficiency and environmental perspective for the suggested combined cycle.

3.8 Working of proposed cycle

Thermodynamic modeling of proposed cycle for different operating conditions using various operating fluids taken into consideration during analysis are studied and compared for the thermodynamic modeling of the low temperature heat source based integrated system. The following assumptions are considered for this analysis (Sulaiman et al., 2023):

- The system is at steady state condition.
- Flow resistance losses in various components are discarded.
- The pressure drops and heat dissipation in the cycle components are neglected.
- The throttling process in expansion valves is isentropic.

The basic idea of current model was first proposed by Keenan et al. in 1950, further it was improved by Huang et al. in 1999 and then Ouzzane & Aidoun in 2003. Entrainment ratio (μ) a vital component of the ejector, establishes the relation between secondary fluid mass rates with respect to that of primary rate exiting the turbine and by using the mass, momentum, and energy equation, the following formulation for the entrainment ratio, which may be written as(Jakończuk et al., 2021):

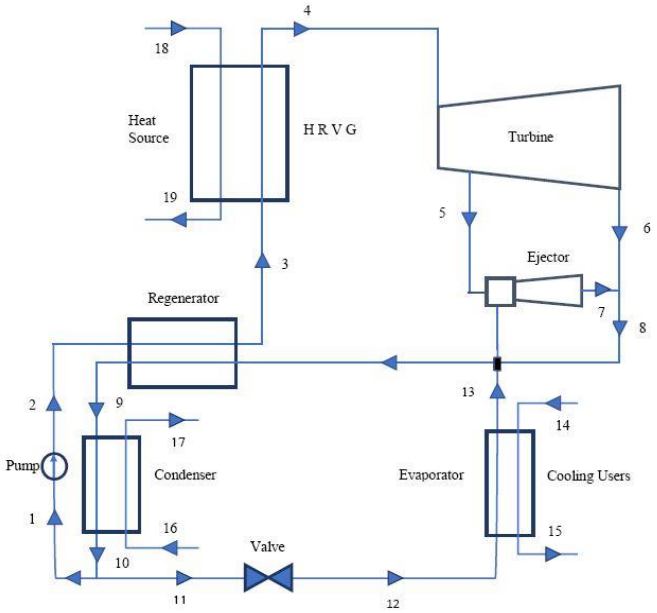

Figure 8: Schematic diagram of combined ORC and ejector refrigeration cycle.

Table 2: Main assumptive parameters of combined cycle (Abam et al., 2019).

Ambient Temperature (K)	298.15
Ambient Pressure (MPa)	0.10135
Turbine's input temperature (K)	373.15
Turbine's input pressure (MPa)	0.6
Turbine's back pressure (MPa)	0.2
Evaporator temperature (K)	263.15
Isentropic efficiency of turbine (%)	85
Isentropic efficiency of pump (%)	80
Extraction ratio	0.35
Heat source mass rate (kg/s)	75
Power/refrigeration	2.5
Mass rate of cooling water (kg/s)	20
Efficiency of the HRVG (%)	100
Variation in temperature at pinch point (C^o)	10.0
Efficiency of the nozzle (%)	90
Efficiency of the mixing chamber (%)	85
Efficiency of the diffuser (%)	85

$$\mu = \sqrt{\frac{\eta_n \eta_m \eta_d (h_{pf,n1} - h_{pf,n2s})}{(h_{mf,ds} - h_{mf,m})}} - 1 \quad (61)$$

$$\dot{m}_{pf} h_{pf,n2} + \dot{m}_{pf} \frac{u^2_{pf,n2}}{2} = \dot{m}_{pf} h_{pf,n1} + \dot{m}_{pf} \frac{u^2_{pf,n1}}{2} \quad (62)$$

$$\eta_n = \frac{h_{pf,n1} - h_{pf,n2}}{h_{pf,n1} - h_{pf,n2s}} \quad (63)$$

$$\dot{m}_{pf} u_{pf,n2} + \dot{m}_{sf} u_{sf,n2} = (\dot{m}_{pf} + \dot{m}_{sf}) u_{mf,ms} \quad (64)$$

$$\frac{1}{2}\left(u^2_{mf,m} - u^2_{mf,ds}\right) = h_{mf,ds} - h_{mf,m} \quad (65)$$

$$\eta_d = \frac{h_{mf,ds} - h_{mf,m}}{h_{mf,d} - h_{mf,m}} \quad (66)$$

$$\mu = \frac{\dot{m}_{sf}}{\dot{m}_{pf}} = \frac{\dot{m}_{13}}{\dot{m}_5} \quad (67)$$

The thermodynamic efficiencies of the proposed cycle as per the thermodynamics first law and it can be presented as follows (Haseli et al., 2008):

$$\eta_{thermal} = \frac{\dot{W}_{net} + \dot{Q}_E}{\dot{Q}_{in}} \quad (68)$$

The ratio of output exergy to the input exergy is known as exergy efficiency (Sotoodeh et al., 2022) (Kumar & Gautam, 2023).

$$\eta_{exergy} = \frac{\dot{W}_{net} + \dot{E}_E}{\dot{E}_{in}} \quad (69)$$

$$\dot{E}_{in} = \dot{Q}_{in}\left(1 - \frac{T_o}{T_{hi}}\right) \quad (70)$$

$$\dot{E}_E = \dot{m}_{sf}[(h_{12} - h_{13}) - T_o(S_{12} - S_{13})] \quad (71)$$

The total exergy destruction is given as

$$\dot{E}D_{Total} = \dot{E}D_{HRVG} + \dot{E}D_T + \dot{E}D_{EJE} + \dot{E}D_{Reg} + \dot{E}D_C + \dot{E}D_P + \dot{E}D_{EV} + ED_E \quad (72)$$

3.5 Thermodynamic modeling of proposed cycle (fig-9) is :

$$\Delta\left[\sum_{out}^{in} m_i\right]=0 \quad (73)$$

$$\Delta\left(\sum_{out}^{in} m_{i.h_i}\right) + \Delta\left[\sum_{out}^{in} Q_j\right] + \Delta\left[\sum_{out}^{in} W_k\right]=0 \quad (74)$$

$$\Delta\left[\sum_{out}^{in} x_{i.} m_i\right]=0 \quad (75)$$

$$T_4=T_0+5 \quad (76)$$

$$m_P = m_4 \times (h_5 - h_4) \quad (77)$$

$$\eta_P = \frac{h_5 - h_4}{h_{isetropic} - h_4} \quad (78)$$

For calculating the amount of mass transfer inside the rectifier, "vmf" denotes the vapor mass fraction and "imf" represents the initial mass of fraction are required. They can be calculating as following (Chen et al., 2016):

$$vmf_R = \frac{x_4 - x_{13}}{x_{10} - x_{13}} \quad (79)$$

$$imf_R = \frac{x_{10} - x_4}{x_{10} - x_{13}} \quad (80)$$

$$W_T = m_8 \times (h_8 - h_9) \quad (81)$$

$$\eta_T = \frac{h_8 - h_9}{h_8 - h_{isetropic}} \quad (82)$$

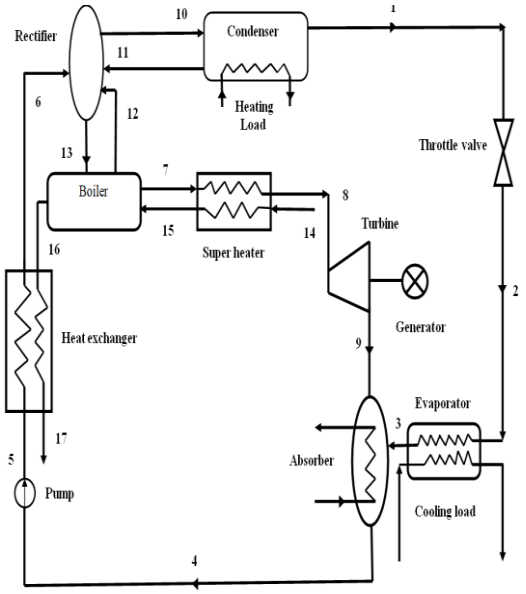

Figure 9: Schematic diagram of the proposed combined power and refrigeration cycle

$$\Delta\left(\sum_{out}^{in} m_i \,.\, h_i\right) + \Delta\left[\sum_{out}^{in} Q_j\right] + \Delta\left[\sum_{out}^{in} W_k\right]=0 \quad (83)$$

$$\Delta\left[\sum_{out}^{in} x_i \,.\, m_i\right]=0 \quad (84)$$

The usable energy output divided by the total energy intake is known as the first law of thermodynamics and is expressed as follows (Fallah et al., 2017):

$$\eta_1 = \frac{W_{net} + Q_E}{Q_{in}} \quad (85)$$

$$\eta_2 = \frac{W_{net} + Q_E}{E_{in}} \quad (86)$$

Where, E_{in} is the heat source fluid exergy and E_{eva} is the exergy associated with refrigeration output which is defined as follows (Yang et al., 2016):

$$E_{in} = m_g[(h_g - h_o) - T_o(s_g - s_o)] \quad (87)$$

$$E_E = m_{evap}[(h_{evap,i} - h_{evap,o}) - T_o(s_{evap,i} - s_{evap,o})] \quad (88)$$

$$\dot{E}D_{Total} = \dot{E}D_P + \dot{E}D_{HE} + \dot{E}D_R + \dot{E}D_B + \dot{E}D_{SH} + \dot{E}D_T + \dot{E}D_C + \dot{E}D_E + \dot{E}D_{TV} + \dot{E}D_A \quad (89)$$

The input simulation data for proposed systems are shown in Table 3.

Table 3: Simulation data of the proposed system

Parameter	Value
Efficiency of heliostat field (η_{field})	0.6428
Number of heliostat (N_{hel})	624
Direct normal irradiation (DNI)	850 W/m^2
Reflective area of each heliostat (A_{hel})	9.45×12.84 m^2
Receiver aperture area (A_{rec})	68.1 m^2
Receiver efficiency (η_{rec})	0.75
Temperature at the inlet of HT (T_4)	800 °C
Isentropic efficiency of helium compressor (η_{HC})	0.89
Effectiveness of heat exchanger (ε)	0.95
Pressure at the inlet of HC	2500 kPa
Isentropic efficiency of helium turbine (η_{HT})	0.93
Isentropic efficiency of ORC turbine (η_{OT})	0.8
Temperature at the inlet of ORC turbine (T_8)	197.2 °C
Pinch point difference in condenser	5 °C
Pinch point difference in WHRU	10 °C
Apparent temperature of the Sun (T_{Sun})	4500 K
Atmospheric temperature (T_0)	25 °C
Atmospheric pressure (P_0)	101.3 kPa
Pressure loss in IHE	2%
Pressure loss in Recuperator/WHRU	1%
Ejector diffuser efficiency	0.95
Ejector mixing efficiency	0.85
Ejector nozzle efficiency	0.9

Trigeneration system has been developed for combined cooling, heating and power generation for the SPT based building applications such as hospitals and hostels. Power is produced through HBC and ORC turbine however for cooling ejector refrigeration has been incorporated. Heat rejection through the condenser has been used for heating purpose. Exergy and energy analysis followed by the parametric analysis were performed for the proposed system.

3.9 **Model validation of proposed cycle**

Fig. 10 illustrates the variation of energy efficiency with respect to the compression pressure ratio (CPR), comparing the results obtained in the present work with those reported by Zhou et al. The graph shows a strong agreement between the two datasets, indicating the accuracy and reliability of the present study's methodology. As observed, energy efficiency increases sharply with CPR up to an optimal value around 2.5, beyond which it begins to decline gradually. This trend suggests that there is an optimal CPR at which the system performs most efficiently, and further increases in pressure ratio lead to reduced efficiency, likely due to higher thermodynamic losses. The close alignment of the two curves further validates the present model and confirms its consistency with previously published results.

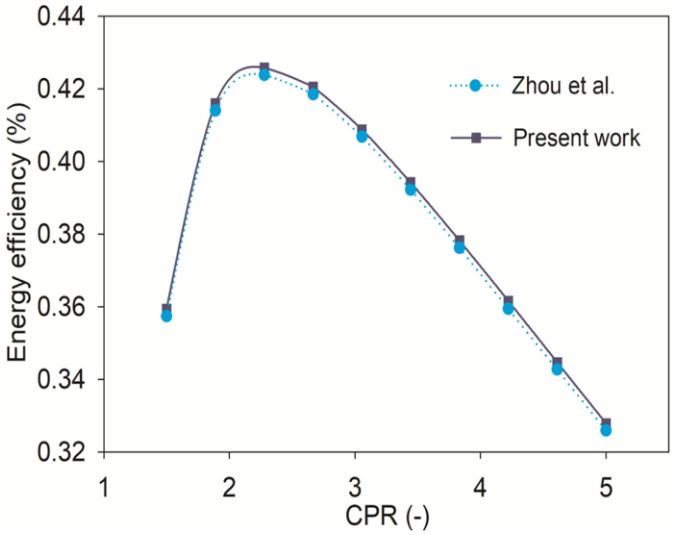

Figure 10: Validation of Brayton cycle

Table 4: Validation of ORC-ERS

Parameters	Present study	Ref. [69]	Deviation (%)
h_9	477.7	474.2	0.73
h_{10}	451.4	451	0.08
h_{11}	447.12	445.4	0.38
h_{12}	221.2	220.1	0.49
h_{13}	220.9	220.1	0.36
h_{14}	376.54	375.5	0.27
h_8	220.97	220.8	0.07
Q_E	60.7	60.4	0.49
$\dot{m}_c$	5.39	5.310	1.5
$\dot{m}_e$	0.391	0.389	0.51
$\dot{W}_{net}$	111.2	110.7	0.004

Table 5: Obtained results from the thermodynamic analysis at the given operating conditions [T_4 = 800°C, CPR=2.3, T_8 = 197.5 °C, DNI=850W/m^2]

Subsystem	Energetic evaluation				Exergetic evaluation			
	Input (kW)	Output (kW)	Loss (kW)	Energy efficiency	Input (kW)	Output (kW)	Loss (kW)	Exergy efficiency
Heliostat field	64358	41369	22989	64.26%	60094	38628	21465	64.27%
Solar receiver	41369	31027	10342	75%	38628	22515	16113	58.28%
HBC	31027	13365	17662	43.07%	22515	13365	9150	59.36%
ORC-ERS	13261	1633	11634	12.26%	3729	1736	1993	46.55%
HBC-ORC-ERS	31027	14998	16035	48.33%	22515	15101	8014	64.40%
Overall plant	64358	14998	49366	23.30%	60094	15101	45593	25.12%

The following conclusions were made from the results in the present research; Combined cycle (HBC-ORC-ERS) energy and exergy efficiency were found 48.33% and 64.4% respectively at the 2.3 of CPR and at the 850 W/m^2 of DNI. The overall plant was obtained 25.12% exergy efficiency, 23.3% energy efficiency and 14998 kW power output, cooling and heating productions are, 8.25 kW and 60.52 kW respectively, at optimum CPR of 2.3. Highest exergy destruction rate was obtained in SPT subsystem (receiver and heliostats) only. It was approximate, 83.20% (37,578 kW) of total exergy destruction (45,593 kW) of the overall plant. The exergoeconomic, environmental analysis of the present research is future scope for the further study.

Table 6: Simulation data of the proposed system

Parameter	Value
Temperature (apparent) of the Sun (T_{Sun})	4500 K
Isentropic efficiency of HT (η_{HT})	0.9
Aperture area of receiver (A_{rec})	68.1 m^2
Heliostat reflecting area (A_{hel})	9.45×12.84 m^2
Receiver efficiency (η_{rec})	0.9
Heliostat counts (N_{hel})	500
Heliostat field efficiency (η_{field})	0.75
Pressure ratio of HC (CPR)	2.5
HC inlet Pressure (P_1)	2500 kPa
Effectiveness of recuperator (ε)	0.9
Isentropic efficiency of HC (η_{HC})	0.88
Highest temperature of HBC (T_4)	850 °C
Direct normal irradiation (DNI)	850 W/m^2
Cascade condenser minimum temperature difference ($\Delta T_{min,cc}$)	8 °C
VCR compressor isentropic efficiency (η_{Comp}) for (0.0467·pressure ratio)	0.8
Absorber temperature (T_{13})	37°C
Condenser inlet temperature (T_{24})	27 °C
Generator temperature (T_{19})	80 °C
Absorber outlet temperature (T_{27})	32 °C
Isentropic efficiency of VAR pump (η_{Pump})	0.9
Effectiveness of SHE (ε_{SHE})	0.7
Cooling load ($\dot{Q}_e$)	30.7 kW
Atmospheric pressure (P_0)	101.3 kPa
Absorber inlet water temperature (T_{26})	27
Condenser outlet water temperature (T_{25})	32
Atmospheric temperature (T_0)	25

3.10 Model validation

Table 7 presents the validation of the cascaded VAR-VCR system by comparing the coefficients of performance (COP) obtained in the current study with reference values reported by Patel et al. (2017). The parameters analyzed include the overall COP of the cascaded system (COP_Cascade), the COP of the vapor absorption refrigeration subsystem (COP_VAR), and the COP of the vapor compression refrigeration subsystem (COP_VCR). The values obtained in this work—0.5393 for COP_Cascade, 0.754 for COP_VAR, and 4.405 for COP_VCR—are closely aligned with the corresponding reference values of 0.54, 0.75, and 4.41, respectively. The estimated percentage errors for these parameters are minimal, ranging from 0.11% to 0.53%, indicating a strong agreement with the reference data. This close match validates the accuracy and reliability of the methodology and results employed in the current study for modeling the cascaded VAR-VCR system.

Table 7: Cascaded VAR-VCR validation

Parameters	Ref. (Patel et al. 2017)	This work	Error estimated (%)
$COP_{Cascade}$	0.54	0.5393	0.12
COP_{VAR}	0.75	0.754	0.53
COP_{VCR}	4.41	4.405	0.11

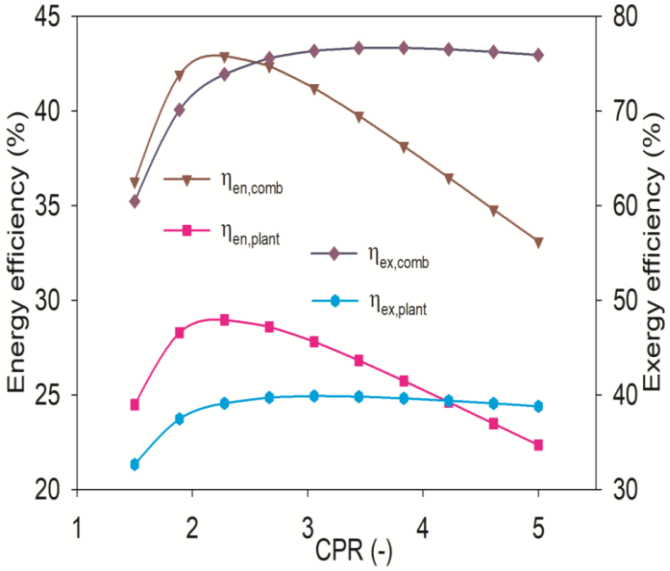

Figure 11: Variation in efficiencies with CPR

Table 8: Energetic and exergetic results

Subsystem	Exergetic evaluation				Energetic evaluation			
	Input (kW)	Output (kW)	Destruction (kW)	Exergy efficiency	Input (kW)	Output (kW)	Loss (kW)	Energy efficiency
Heliostat field	48152	36114	12038	75%	51569	38676	12893	75%
Solar receiver	36114	25389	10725	70.30%	38676	34809	3868	90%
Trigeneration system	25389	19039	6350	74.98%	34809	14865	19944	42.7%
Overall plant	48152	19039	29113	39.53%	51569	14865	36704	28.82%

Table 9: Performance compression with previous studies

Systems	$\eta_{receive}$	η_{field}	$\eta_{field} \times \eta_{receiver}$	DNI (kW/m^2)	η_{cycle} (%)	$\eta_{ex,plant}$ (%)	$\eta_{en,plar}$ (%)
Regenerative supercritical Rankine cycle (Xu et al. 2011)	0.9	0.75	--	0.8	42.1	27.4	25.7
Regenerative Rankine cycle (Xu et al. 2011)	0.9	0.75	--	0.8	37.9	24.5	22.9
Present plant	0.9	0.75	--	0.8	42.79	39.53	28.82
Combined tCO_2-ORC (Chacartegui et al. 2021)	N.A	N.A	0.62	1	43.96	N.A	27.14
sCO_2 cycle (Chacartegui et al. 2021)	N.A	N.A	0.62	1	42.48	N.A	26.23
Present plant	--	--	0.62	1	46.32	42.02	31.89

In this work, a Brayton cycle based on helium is used to provide an effective tri-generation system for a SPT facility. Cascade VAR-VCR generates low temperature cooling and heating by utilizing waste heat from the Brayton cycle. To find out how sensitive the plant's independent variables were to the performance parameters, a parametric analysis was conducted. According to the findings, the SPT-based plant (SPT-HBC-VAR-VCR) generates exergy and energy efficiencies of 39.53% and 28.82% respectively under typical operating conditions. COPs were used to calculate the heating and cooling performance. Calculations revealed that COP_c and COP_h were, respectively, 0.5391 and 1.539. The trigeneration system was obtained as 74.98% of exergy efficiency. However, solar sub-system accounts for the largest portion of the plant's total exergy destruction, or about 78.18% (22763 kW). In addition, the current system generated heating effect for the applications like domestic water heating etc. and cooling at low temperature for food preservation etc.

Table 10: Simulation data of the proposed system

Parameter	Value
Receiver efficiency (η_{rec})	0.75 [89]
Receiver aperture area (A_{rec})	68.1 m^2 [75]
Heliostat field efficiency (η_{field})	0.6428 [75]
Each heliostat area (A_{hel})	9.45×12.84 m^2[75,80]
Number of heliostat (N_{hel})	624 [75]
Solar irradiation (DNI)	850 W/m^2 [80]
T1 inlet temperature (T_4)	850 ℃ [89]
C1 inlet pressure (P_1)	2500 kPa [75]
Isentropic efficiency of T1 (η_{T1})	0.93 [69,77]
Isentropic efficiency (η_{T2})	0.8 [75]
Maximum temperature of ORC (T_9)	197.4 °C
Effectiveness of heat exchanger (ε)	0.95 [77]
Condenser pinch	5 ℃ [75]
HRVG pinch	10 ℃ [75, 80]
Cascade condenser temperature (T_{CC})	-10 °C
Evaporator temperature (T_{EVAP})	-40 °C
Sun apparent temperature (T_{Sun})	4500 K [44]
Ambient temperature (T_0)	25 °C
Atmospheric pressure (P_0)	101.3 kPa
Mixing efficiency of ejector	0.85 [45]
Nozzle efficiency of ejector	0.9 [45]
Ejector diffuser efficiency	0.95 [45]

3.11 Model validation

Table 11: ORC-ERS Validation

Parameters	Present study	Ref. [69]	Deviation (%)
h_9	477.7	474.2	0.73
h_{10}	451.4	451	0.08
h_{11}	447.12	445.4	0.38
h_{12}	221.2	220.1	0.49
h_{13}	220.9	220.1	0.36
h_{14}	376.54	375.5	0.27
h_8	220.97	220.8	0.07
Q_E	60.7	60.4	0.49
$\dot{m}_c$	5.39	5.310	1.5
$\dot{m}_e$	0.391	0.389	0.51
$\dot{W}_{net}$	111.2	110.7	0.004

Table 12: Obtained results at base conditions

Parameters	SPT-HBC	HBC-ORC-ERS-VCR	SPT- HBC-ORC-ERS-VCR
Energy efficiency (%)	30.15	89.86	60.66
Exergy efficiency (%)	32.29	67.55	35.55
Output (kW)	15547	15585	15585
Heating effect (kW)	-	14967	14967
Cooling effect (kW)	-	730	730
Exergy destruction (kW)	32603	15625	31033
Total output energy (kW)	15547	31282	31282

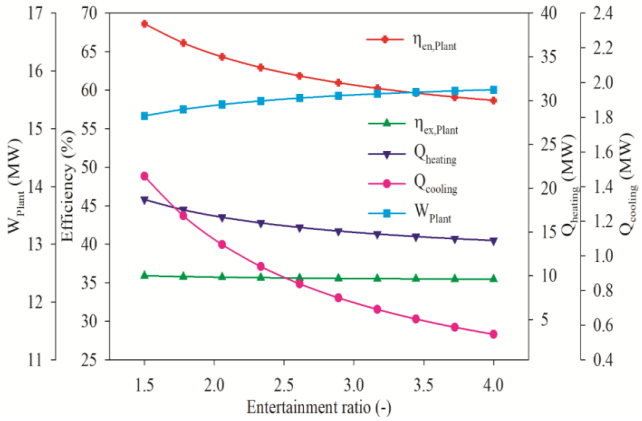

Figure 12: Effect of the Entertainment ratio on performance of the plant

Table 13: Input data for above systems

Ambient temperature (°C)	20
Ambient pressure (MPa)	0.10135
Turbine's inlet pressure (MPa)	2.5
Turbine's inlet temperature (°C)	285.0
Isentropic efficiency of the turbine (%)	85
Refrigeration temperature (°C)	−25
Heat source temperature (°C)	300
Heat source mass rate (kg/s)	20
Pinch point temperature difference (°C)	15
Isentropic efficiency of the pump (%)	70
Ammonia mass fraction of basic solution	0.34

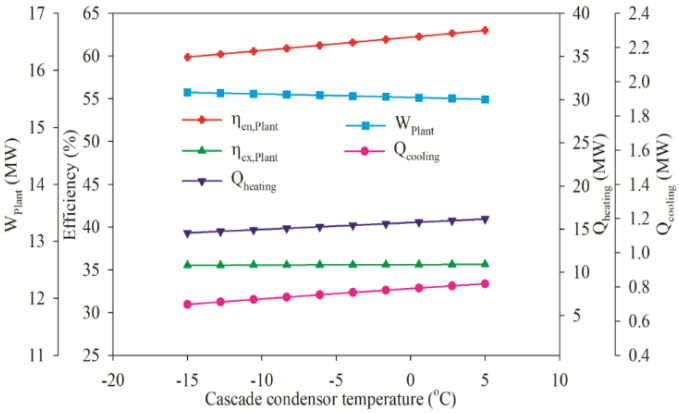

Figure 13: Effect of temperature of cascade condenser on plant performance

In the present work a solar based trigeneration system is proposed. The ORC, ERS, and VCR system has been implemented to the conventional SPT-HBC system to enhance the performance of the proposed plant. The exergy and energy analysis has been performed using the computational software EES. The following conclusions were made from the analysis; The overall proposed solar plant (SPT-HBC-ORC-ERS-VCR) obtained the energy efficiency and exergy efficiency of as 60.66% and 35.55% respectively. However, the net work out was obtained as 15585 kW. The Heating and cooling effects were obtained as 14967 kW and 730 kW for the industrial application and food storage application respectively. The exergy efficiency of the conventional plant (SPT-HBC) was obtained as 32.29%. Exergy efficiency of the proposed system is 10.09% higher than conventional plant.

Table 14: Validation of the computed results of current work

Parameters	Comparison for binary ammonia-water mixture	
	This work	Mohtaram et al. (2017)
Heat source inlet temperature (K)	573.15	573.15
Turbine inlet temperature (K)	558.15	558.15
Evaporator temperature (K)	248.15	248.15
(a) Results		
Turbine work (KW)	616.693	614.3
Pump work (KW)	5.971	2.774
Absorber heat rejection (KW)	3244.35	3241

Table 15: Main assumptive parameters considered for the analysis (Mohtaram et al., 2017).

Condenser heat rejection (KW)	458.59	458.59
Refrigeration output (KW)	224.947	225.5
Boiler heat input (KW)	2605.47	2612
Superheat input (KW)	236.4	232.1
Heat exchanger heat input (KW)	1272.6	1282
Net power output (KW)	610.722	614.3
Net power and Refrigeration output (KW)	835.669	839.8
Heat input (KW)	4090.81	4091.82
Exergy input (KW)	1846.34	1846.34
Thermal efficiency (%)	20.25	20.35
Exergy efficiency (%)	35.56	35.68

Table 13 outlines the baseline input parameters for the thermodynamic analysis. The system operates under ambient conditions of 20°C and 0.10135 MPa pressure. The turbine inlet is maintained at a relatively high pressure of 2.5 MPa and a temperature of 285°C, which enables sufficient energy extraction during expansion. The isentropic efficiency of the turbine is set at 85%, indicative of a reasonably efficient expansion process. The refrigeration temperature is maintained at -25°C, representing low-temperature cooling demand, while the heat source temperature for the generator is assumed to be 300°C with a mass flow rate of 20 kg/s. The pinch point temperature difference, which is crucial in determining the minimum temperature difference in the heat exchangers to avoid operational issues, is taken as 15°C. The isentropic efficiency of the pump, at 70%, reflects moderate energy losses in liquid compression. Finally, the ammonia mass fraction of the basic solution is set at 0.34, a typical value for optimal working fluid concentration in ammonia-water absorption systems. Table 14 presents the validation of the computational model against results from Mohtaram et al. (2017). Identical inlet conditions were used for comparison, including a heat source temperature of 573.15 K (300°C), turbine inlet temperature of 558.15 K, and evaporator temperature of 248.15 K. The turbine work output in the current study is 616.693 kW, closely matching the 614.3 kW reported by Mohtaram et al., indicating a high level of accuracy. However, a slight discrepancy is noted in the pump work, with the present model yielding 5.971 kW compared to 2.774 kW, possibly due to different assumptions in isentropic pump efficiency. The absorber heat rejection in the current analysis (3244.35 kW) is nearly identical to the reference value (3241 kW), reinforcing the validity of the thermal interactions modeled. Table 15 expands on the main assumptive parameters and further compares results from the current analysis with Mohtaram et al. The condenser heat rejection is consistent at 458.59 kW in both studies. The refrigeration output also aligns well, with a negligible difference between 224.947 kW (this work) and 225.5 kW (Mohtaram et al.). Boiler heat input, superheat input, and heat exchanger contributions also show close agreement, supporting the integrity of the energy balances. The net power output in this work is slightly lower at 610.722 kW versus 614.3 kW.

Table 16: Simulation results at base conditions

State	Temperature (K)	Pressure (bar)	Dryness	Enthalpy (kj/kg)	Entropy (kJ/kgK)	Mass flow rate (kg/s)	Mass fraction (x)
1	298.15	25	0	118.127	0.4141	0.193084	0.9999
2	245.15	1.1941	0.17169	118.127	0.5373	0.193084	0.9999
3	268.15	1.1941	1	1283.15	5.2835	0.193084	0.9999
4	298.15	1.1941	0	-96.75	0.2818	1.46725	0.34
5	298.57	25	0	-92.68	0.2811	1.46725	0.34
6	432.24	25	0.17575	763.25	2.5541	1.46725	0.34
7	488.5	25	1	2538	6.202	1.27416	0.24
8	558.15	25	1	2745.5	6.537	1.27416	0.24
9	369.25	1.1941	0.93029	2240.41	6.8055	1.27416	0.24
10	334.69	25	1	1305.72	4.0322	0.386168	0.9999
11	298.15	25	0	118.127	0.4141	0.193084	0.9999
12	486.5	25	1	2539.24	6.2083	0.026106	0.24
13	432.4	25	0	541.8	1.96343	1.30027	0.24

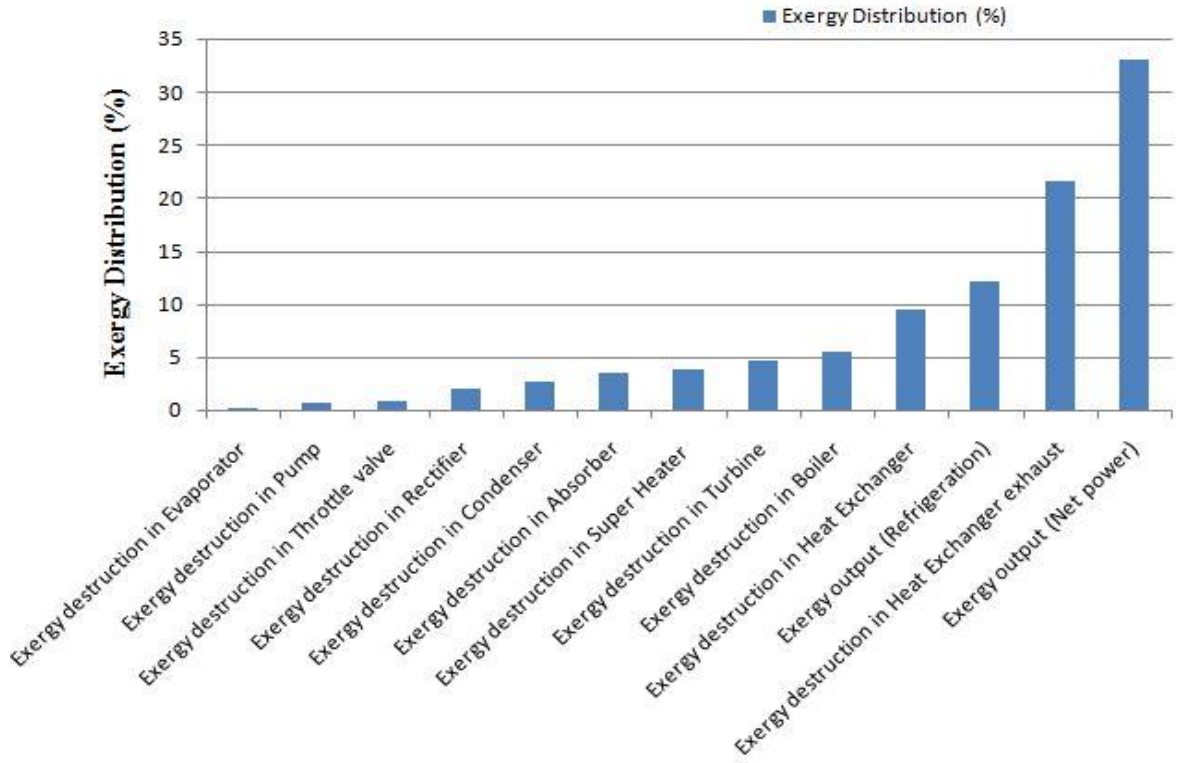

Figure 14: Distribution of input heat source energy of solar based trigeneration system.

The considered cycle in this investigation applies a binary mixture of water and ammonia as its working fluid and is a combination of both absorption refrigeration and Rankine cycles. Parametric analysis of the thermodynamic parameters effects on the system performance shows that the temperatures of heat source, ambient, refrigeration the turbine as well as inlet pressure have major effects on refrigeration and net power output, thermal, and exergy efficiencies.

Due to the structure and operating units such as evaporator, ejector and so on, the considered cycle in this study can produce higher refrigeration when it is compared with the other combined power and refrigeration cycles. From the results it can be concluded that a gradual growth at turbine inlet pressure causes an eventual rise in energy efficiency and exergy efficiency of the combined cycle. Heat exchanger exhaust is the biggest source of exergy destruction followed by the heat exchanger, boiler, turbine, super heater, absorber, condenser and rectifier respectively.

3.12 Model validation

Table 17 details the validation of the computational model against the study by Dai et al. (2009) for R-123 as the working fluid. Both studies use identical input conditions: a

heat source inlet temperature of 413 K, condenser temperature of 293 K, and evaporator temperature of 263 K. The results show strong agreement between the two works. For example, the total heat input in the heat recovery vapor generator (HRVG) is 1262 kJ/kg in the current study compared to 1246.96 kJ/kg by Dai et al., indicating minimal deviation. The ejector's entrainment ratio, a key parameter that determines the suction capability, is very close (0.394 vs. 0.389). The computed turbine work (116.18 kJ/kg) and net power output (113.53 kJ/kg) are slightly higher but within an acceptable range when compared to Dai's values (114.14 and 110.69 kJ/kg respectively). Similarly, the refrigeration output (62.34 vs. 60.44 kJ/kg) and thermal (13.67%) and exergy (22.75%) efficiencies show minimal deviation, which strongly supports the validity of the present computational model. Minor differences could be attributed to variations in numerical methods or assumptions related to thermophysical properties, but overall, the model proves reliable. Table 18 expands the analysis by comparing the combined cycle performance for six different refrigerants: R-123, R-124, R-141b, R-290 (propane), R-134a, and R-152a. Various thermodynamic and exergetic parameters are presented for a comparative assessment. Among the refrigerants, R-152a produces the highest net power output (78.59 kW) and thermal efficiency (7.656%), with the highest exergy efficiency at 19.78%. This indicates its potential for efficient energy utilization in the combined cycle. R-290 also performs well, showing a thermal efficiency of 18.546% and exergy efficiency of 13.74%, making it a strong candidate for applications requiring both power and cooling. The parameter μ, which may represent a design-specific dimensionless factor, varies across refrigerants, affecting mass flow rate (ṁ), which directly influences energy exchange. For instance, R-134a has the highest mass flow rate (6.405 kg/s), and consequently, the highest HRVG heat destruction (ĖḊ_HRVG) at 92.62 kW, suggesting more intense thermal processing. R-123, while producing moderate values in terms of power output (51.85 kW) and cooling (20.52 kW), shows a balanced performance with relatively high thermal efficiency (17.057%) and moderate exergy efficiency (12.85%). The exergy destruction rates (ĖḊ) across key components (HRVG, turbine, ejector, regenerator, condenser, pump, evaporator, and expansion device) provide insights into where irreversibilities dominate. For example, R-134a and R-152a exhibit higher ĖḊ values in the regenerator and condenser, indicating significant losses there. The exergy output from the evaporator (Ė_E) is highest for R-152a, aligning with its high cooling output.

Table 17: Validation of the computed results of current work

Parameters	Comparison for R-123	
	Present work	Dai et al.(2009)
Heat source inlet temperature (K)	413	413
Condenser temperature (K)	293	293
Evaporator temperature (K)	263	263
Total heat in HRVG (Kj/Kg)	1262	1246.96
Ejector's entrainment ratio	0.394	0.389
Pump work (Kj/Kg)	3.48	3.45
Turbine's work (kj/Kg)	116.18	114.14
Net Power output (kj/Kg)	113.53	110.69
Refrigeration output (kj/Kg)	62.34	60.44
$\dot{W}_{net}/\dot{Q}_{in}$	8.56	8.88
$\dot{Q}_E/\dot{Q}_{in}$	4.68	4.85
Refrigeration/Power ratio	0.36	0.35
Thermal efficiency (%)	13.67	13.72
Exergy efficiency (%)	22.75	22.2

Table 18: Combined cycle performance using six different refrigerants

Variable	Unit	R-123	R-124	R-141b	R-290	R-134a	R-152a
μ	-	0.1261	0.1592	0.1023	0.1247	0.1436	0.1238
ṁ	Kgs^{-1}	2.037	4.053	1.642	4.235	6.405	4.562
$\dot{E}\dot{D}_{HRVG}$	KW	16.45	37.64	13.32	47.84	92.62	96.54
$\dot{E}\dot{D}_{T}$	KW	9.546	9.435	9.74	9.68	10.86	13.64
$\dot{E}\dot{D}_{EJE}$	KW	10.384	14.73	10.42	10.27	18.78	18.52
$\dot{E}\dot{D}_{Reg}$	KW	1.423	9.123	1.344	11.416	40.72	27.46
$\dot{E}\dot{D}_{C}$	KW	6.304	9.86	6.324	7.68	14.23	14.32
$\dot{E}\dot{D}_{P}$	KW	0.1623	0.213	0.1604	0.1468	0.0351	0.1065
$\dot{E}\dot{D}_{EV}$	KW	0.2536	0.34	0.2242	0.4247	0.6201	0.6271
$\dot{E}\dot{D}_{E}$	KW	0.2351	0.3263	0.0713	0.2723	0.4715	0.4423
$\dot{W}_{T}$	KW	52.84	54.78	57.46	56.75	61.75	79.38
$\dot{W}_{P}$	KW	0.986	1.524	0.9547	1.81	0.2964	0.7846
$\dot{W}_{net}$	KW	51.854	53.256	56.5053	54.94	61.453	78.59
$\dot{Q}_{E}$	KW	20.52	21.43	22.42	37.47	24.85	31.72
$\dot{Q}_{in}$	KW	422.45	695.68	451.47	501.87	1305.87	1428.68
$\dot{E}_{E}$	KW	1.732	2.232	2.134	2.896	2.265	2.745
$\eta_{thermal}$	%	17.057	10.652	17.292	18.546	6.486	7.656
η_{exergy}	%	12.85	12.47	13.57	13.74	15.24	19.78

The current study examines the combined ORC and ejector refrigeration cycle applying environmentally friendly refrigerants as the operating fluids. The proposed cycle's performance including its exergy output, exergy efficiency, entrainment ratio, thermal efficiency and total exergy destruction is examined using first law and second law analysis at critical input variables including evaporator temperature, turbine input temperature and heat source fluid temperature. The Distribution of input heat source energy of integrated combined cycle is shown in Fig-15

.

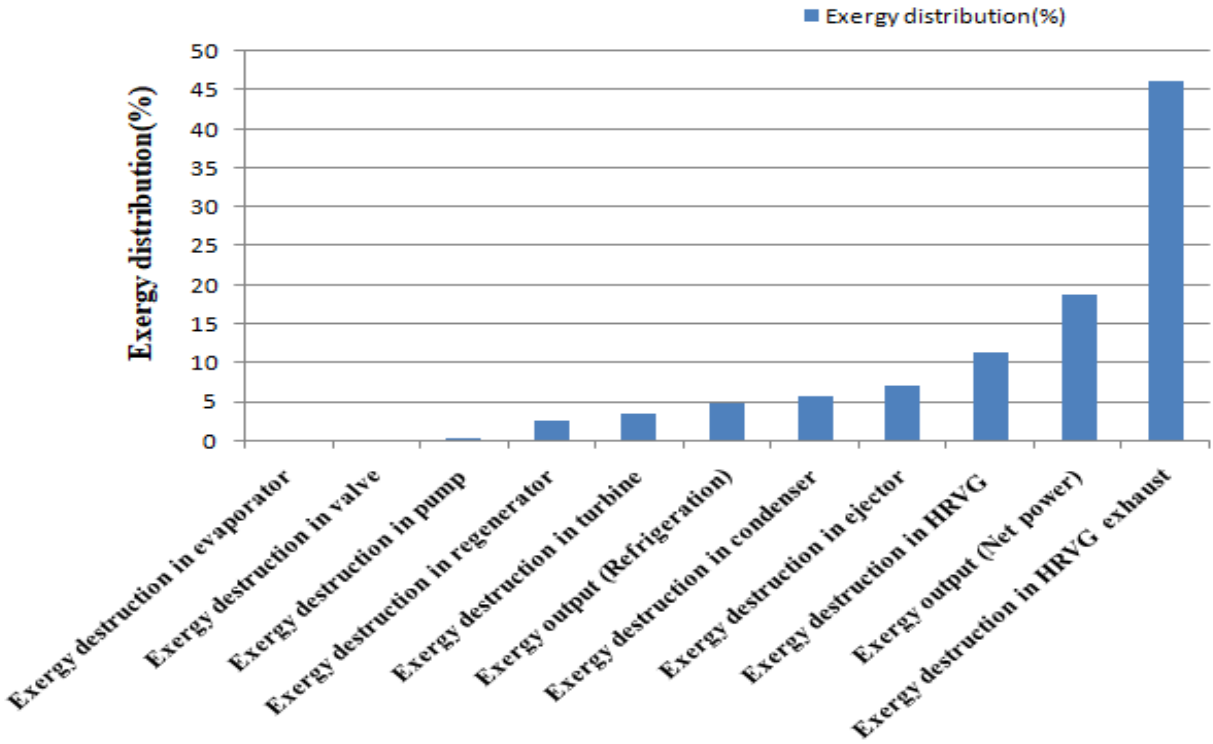

Figure 15: Distribution of input heat source energy of integrated combined cycle

From the above discussion, the following are the primary conclusions:

As the evaporator temperature rises, refrigeration output increases while exergy efficiency and entrainment ratio decline. The thermal efficiency and exergy efficiency increases with the rise in temperature at the turbine input and at and heat source fluid temperature. The differences in molecular structure, operating conditions, and environmental impact contribute to the variations in exergy efficiency between R-152a and R-123, with R-152a generally having higher efficiency due to its favorable thermodynamic properties and lower environmental impact. Among the several operating fluids examined in this article, R-152a and R-134a are the most appropriate from the perspectives of exergy efficiency and environmental impact for the suggested combined cycle. The outcomes of the study help optimally design the combined power, cooling, and heating system by low temperature sources using working fluid as environment friendly refrigerants. In the future, detailed studies on this system are required, particularly experimental examination to determine the specific utility of the suggested cycle to exploit various low temperature heat sources. In this investigation the detailed energy and exergy analysis of a solar based trigeneration system integrated ejector cooling, heating and power cycle using various eco-friendly refrigerants, combined power and cascaded compression-absorption system, combined power and cascaded ejector-vapor compression refrigeration system and combined power-absorption refrigeration cycle with heating process employed with helium Brayton cycle organic Rankine cycle for recovering the waste heat have been presented. Based on the theoretical studies and investigations, the major outcomes of the present work were obtained solving mathematical equations by using computational technique EES are summarized below:

3.13 SPT driven combined HBC and ORC with ejector refrigeration trigeneration system

Addition of ejector refrigeration cycle with ORC produces power and cooling simultaneously. Thermal efficiency and exergy efficiency of the HBC-ORC-ERS cycle improved by 5.26 % and 5.04%, respectively, by recovering waste heat using bottoming ORC. The net power output and both efficiencies of the combined cycle improved continuously with solar irradiation, helium turbine inlet temperature, ORC turbine inlet temperature and evaporator temperature. In addition, through the WHRU, ORC-ERS unit was able to

absorb 13,261 kW of waste heat out of 31,027 kW of solar heat absorbed by the HBC. Combined cycle/trigeneration system (HBCORC- ERS) energy and exergy efficiency were found 48.33% and 64.4% respectively at the 2.3 of CPR and at the 850W/m^2 of DNI. The overall plant was obtained 25.12% exergy efficiency, 23.3% energy efficiency and 14,998kW power output, cooling and heating productions are, 8.25 kW and 60.52 kW respectively, at optimum CPR of 2.3. Only the receiver and heliostats in the SPT subsystem had the highest rate of exergy destruction. It represented roughly 83.20% (37,578 kW) of the plant's total exergy destruction (45,593 kW). Advantage of the present analysis is to develop the efficient power system to generate the carbon free power, heating and cooling in future with fewer components compared to previous research. SPT based proposed trigeneration system performed better than the other SPT based similar system. The exergoeconomic, environmental analysis of the present research is future scope for the further study. In order to achieve better performance, proper working fluid selection is needed.

3.14 SPT based combined HBC integrated compression-absorption trigeneration system

Integration of a two different cascaded refrigeration cycle with and power cycle produces cooling at two different temperatures along power simultaneously. The SPT-based plant (SPT-HBC-VAR-VCR) generates exergy and energy efficiencies of 39.53% and 28.82% respectively under typical operating conditions. COPs were used to calculate the heating and cooling performance. Calculations revealed that COP_c and COP_hwere, respectively, 0.5391 and 1.539. The trigeneration system was obtained as 74.98% of exergy efficiency. However, solar sub-system accounts for the largest portion of the plant's total exergy destruction, or about 78.18% (22763 kW). Furthermore, the parametric evaluation revealed that efficiency of receiver and heliostat, CPR, HT turbine inlet temperature, temperature of evaporator and generator, all had a significant impact on the performance of the plant. In addition, the current system generated heating effect for the applications like domestic water heating etc. and cooling at low temperature for food preservation etc. Furthermore, a comparative analysis with relevant previous studies has shown that the proposed CCHP system outperforms systems based on supercritical CO_2 cycles and the Rankine cycles. Proposed plant is limited to operate at peak load conditions due to absence of thermal energy storage system. The economic feasibility as well as optimization study of the present proposed work can be work for future research.

3.15 SPT based combined HBC-ORC integrated ejector-compression trigeneration system

The overall proposed solar plant (SPT-HBC-ORC-ERS-VCR) obtained the energy efficiency and exergy efficiency of as 60.66% and 35.55% respectively. However, the net work out was obtained as 15585 kW. Heating and cooling effects were obtained as 14967 kW and 730 kW for the industrial application and food storage application respectively. The exergy efficiency of the conventional plant (SPT-HBC) was obtained as 32.29%. Exergy efficiency of the proposed system is 10.09% higher than conventional plant. The high heat loss obtained in heliostats field and the central receiver. This due to much useful energy obtained from the proposed system in terms of heating, cooling effects and power generation.

It can be seen that overall proposed solar plant's exergy efficiency is lower than the trigeneration system due the higher irreversibilities were present in the SPT components i.e.in central receiver and the heliostats field. The energy, exergy efficiency and the net work production were decreased from 68.63% to 58.67%, 35.91% to 35.46% and 15222 kW to 15675 kW respectively as the entertainment ratio increased from 1.5 to 4. However, the heating and cooling loads decreased from 18709 kW to 14301kW and 1459 kW 547.1kW respectively, as the entertainment ratio increased from 1.5 to 4. It can be seen this ratio much affected the cascaded ejector-VCR system rather than the topping cycle performance.

3.16 Combined power-absorption and heating cycle integrated trigeneration system

Temperatures of heat source, ambient, refrigeration the turbine as well as inlet pressure and the concentration of ammonia base solution (working fluid) have major effects on refrigeration output, the net output power, thermal, and exergy efficiencies.

Due to the structure and operating units such as evaporator, ejector and so on, the considered cycle in this study can produce higher refrigeration when it is compared with the other combined power and refrigeration cycles. From the results it can be concluded that a gradual growth at turbine inlet pressure causes an eventual rise in energy efficiency and exergy efficiency of the combined cycle. Heat exchanger exhaust is the biggest source of exergy destruction followed by the heat exchanger, boiler, turbine, super heater, absorber, condenser and rectifier respectively.

3.17 Combined power, heating and cooling cycle using low temperature heat source with various eco-friendly refrigerants integrated trigeneration system

As the evaporator temperature rises, refrigeration output increases while exergy efficiency and entrainment ratio decline. The thermal efficiency and exergy efficiency increases with the rise in temperature at the turbine input and at and heat source fluid temperature. The differences in molecular structure, operating conditions, and environmental impact contribute to the variations in exergy efficiency between R-152a and R-123, with R-152a generally having higher efficiency due to its favorable thermodynamic properties and lower environmental impact. Among the several operating fluids examined in this article, R-152a and

R-134a are the most appropriate from the perspectives of exergy efficiency and environmental impact for the suggested combined cycle. It is noted that out of 100% input energy, approximately 18.667% and 4.857% of the above-mentioned energy are converted in power and refrigeration production respectively, while the leftover energy is losses to the environment as a result of entropy generation in the integrated system's components. It has been noted that the HRVG exhaust experiences the highest exergy loss, which is 46.12%. The percentage of exergy destroyed across the HRVG, ejector, and condenser is 11.324%, 6.978% and 5.65% respectively. The percentage of exergy destruction on remaining parts of the cycle was below one. The second law analysis's results, which were used to determine the component's local irreversibility, show that the HRVG and ejector require more attention because they were been identified as the primary sources of losses within the system.

4. Conclusion

Following conclusions were drawn from present investigation

- SPT based proposed trigeneration system performed better than the other SPT based similar system. In order to achieve better performance, proper working fluid selection is needed.
- The proposed CCHP system outperforms systems based on supercritical CO_2 cycles and the Rankine cycles and the CCHP system is limited to operate at peak load conditions due to absence of thermal energy storage system.
- (iii)For SPT based combined HBC-ORC integrated ejector-compression trigeneration system, **the** overall proposed solar plant’s exergy efficiency is lower than the trigeneration system due the higher irreversibility were present in the SPT components i.e.in central receiver and the heliostats field.
- ((iv) In the Combined power-absorption and heating cycle integrated trigeneration system, the only ammonia water mixture can be used in the combined power and refrigeration cycle amongst binary working fluids as refrigerants. As other fluids when divided to refrigerant and absorbent, the fluids have to act as the absorbent and to leave salty residues or sediments behind, once they pass through the turbine. For this reason, there fluids have no practical use in turbine.
- (v) The optimally design the combined power, cooling, and heating system by low temperature sources using working fluid as environment friendly refrigerants. In the future, detailed studies on this system are required, particularly experimental examination to determine the specific utility of the suggested cycle to exploit various low temperature heat sources.

References

[1] Yoro, K. O. and Daramola, M. O. CO2 emission sources, greenhouse gases, and the global warming effect. In Advances in carbon capture, pages 3–28. Elsevier, 2020.

[2] Liu, Z., Ciais, P., Deng, Z., Lei, R., Davis, S. J., Feng, S., Zheng, B., Cui, D., Dou, X., Zhu, B., et al. Near-real-time monitoring of global CO2 emissions reveals the effects of the COVID-19 pandemic. Nature communications, 11(1): 1–12, 2020.

[3] Ibrahim, O., Fardoun, F., Younes, R., and Louahlia-Gualous, H. Review of water-heating systems: General selection approach based on energy and environmental aspects. Building and Environment, 72:259–286, 2014.

[4] Ahmad, T. and Zhang, D. A critical review of comparative global historical energy consumption and future demand: The story told so far. Energy Reports, 6:1973–1991, 2020.

[5] Smith, L. V., Tarui, N., and Yamagata, T. Assessing the impact of COVID-19 on global fossil fuel consumption and CO2 emissions. Energy economics, 97: 105170, 2021.

[6] Ahmadi, P. Modeling, analysis and optimization of integrated energy systems for multi generation purposes. PhD thesis, University of Ontario Institute of Technology, 2013.

[7] Spahni, R., Chappellaz, J., Stocker, T. F., Loulergue, L., Hausammann, G., Kawamura, K., Fluckiger, J., Schwander, J., Raynaud, D., Masson-Delmotte, V, Atmospheric methane and nitrous oxide of the late pleistocene from antarctic ice cores. Science, 310 (5752):1317–1321, 2005.

[8] Ahmadi, P., Rosen, M. A., and Dincer, I. Greenhouse gas emission and exergo environmental banalyses of a trigeneration energy system. International Journal of Greenhouse Gas Control, 5(6):1540–1549, 2011.

[9] Al Moussawi, H., Fardoun, F., and Louahlia-Gualous, H. Review of trigeneration technologies: Design evaluation, optimization, decision-making, and selection approach. Energy Conversion and Management, 120:157–196, 2016.

[10] Al-Sulaiman, F. A., Hamdullahpur, F., and Dincer, I. Trigeneration: A comprehensive review based on prime movers. International journal of energy research, 35(3):233–258, 2011.

[11] Anvari, S., Jafarmadar, S., and Khalilarya, S. Proposal of a combined heat and power plant hybridized with regeneration organic Rankine cycle: Energy- Exergy evaluation. Energy Conversion and Management, 122:357–365, 2016.

[12] Boyce, M. Combined cycle power plants. In Combined cycle systems for nearzero emission power generation, pages 1–43. Elsevier, 2012.

[13] Garofalo, E., Bevione, M., Cecchini, L., Mattiussi, F., and Chiolerio, A. Waste heat to power: Technologies, current applications, and future potential. Energy Technology, 8(11):2000413, 2020.

[14] Johnson, I., Choate, W. T., and Davidson, A. Waste heat recovery. Technology and opportunities in US industry. Technical report, BCS, Inc., Laurel, MD (United States), 2008.

[15] Jouhara, H., Khordehgah, N., Almahmoud, S., Delpech, B., Chauhan, A., and Tassou, S. A. Waste heat recovery technologies and applications. Thermal Science and Engineering Progress, 6:268–289, 2018.

[16] Al-Sulaiman, F. Thermodynamic Modeling and Thermoeconomic Optimization of Integrated Trigeneration Plants Using Organic Rankine Cycles. PhD thesis, University of Waterloo, 2010.

[17] Jouhara, H., Khordehgah, N., Almahmoud, S., Delpech, B., Chauhan, A., and Tassou, S. A. Waste heat recovery technologies and applications. Thermal Science and Engineering Progress, 6:268–289, 2018.

[18] Wang, A., Wang, S., Ebrahimi-Moghadam, A., Farzaneh-Gord, M., and Moghadam, A. J. Techno- economic and techno-environmental assessment and multi-objective optimization of a new CCHP system based on waste heat recovery from regenerative Brayton cycle. Energy, 241:122521, 2022.

[19] Javadi, M. A., Abhari, M. K., Ghasemiasl, R., and Ghomashi, H. Energy, exergy and exergy- economic analysis of a new multigeneration system based on double-flash geothermal power plant and solar power tower. Sustainable Energy Technologies and Assessments, 47:101536, 2021.

[20] Moghimi, M., Emadi, M., Ahmadi, P., and Moghadasi, H. 4E analysis and multi-objective optimization of a CCHP cycle based on gas turbine and ejector refrigeration. Applied Thermal Engineering, 141:516–530, 2018.

[21] Kim, Y. M., Sohn, J. L., Yoon, E. S. Supercritical CO2 Rankine cycles for waste heat recovery from gas turbine, Energy 118 (2016) 893-905.

[22] Kim, M.S., Y. Ahn,B. Kim, and J.I. Lee. Study on the supercritical CO2 power cycles for landfill gas firing gas turbine bottoming cycle. Energy 111 [2016]: 893-09.

[23] Park, S. H., Kim, J. Y., Yoon, M. K., Rhim, D. R., Yeom, C. S. Thermodynamic and economic investigation of coal-fired power plant combined with various supercritical CO2 Brayton power cycle, Applied Thermal Engineering 130 (2018) 611–623.

[24] Li, L., Ge, Y. T. Luo, X., Tassou, S. A. Experimental analysis and comparison betweenCO2 transcritical power cycles and R245fa organic Rankine cycles for low-grade heat power generations, Applied Thermal Engineering 136 (2018) 708–717.

[25] Neises, T., Turchi, C. Supercritical carbon dioxide power cycle design and configuration optimization to minimize levelized cost of energy of molten salt power towers operating at 650°C, Solar Energy 181 (2019) 27–36.

[26] Fan, G., H. Li, Y. Du, K. Chen, S. Zheng, and Y. Dai. 2020. Preliminary design and part-load performance analysis of a recompression supercritical carbon dioxide cycle combined with a transcritical carbon dioxide cycle, Energy Conversion and Management 212:112758.

[27] Khatoon, S. and M. Kim.2020.Performance analysis of carbon dioxide based combined power cycle for concentrating solar power. Energy Conversion and Management 20. doi:10.1016/j.enconman.2019.112416.

[28] Yu, W., Q. Gong, D. Gao, G. Wang, H. Su, and X. Li. 2020. Thermodynamic Analysis of Supercritical Carbon Dioxide Cycle for Internal Combustion Engine Waste Heat Recovery. Processes. 8:216. doi: 10.3390/pr8020216.

[29] Tchanche, B.F., Quoilin, S., Declaye, S., Papadakis, G. and Lemort V., "Economic Optimization of Small Scale Organic Rankine Cycles," In: 23rd International conference on efficiency, cost, optimization, simulation and environmental impact of energy systems (ECOS), Lausanne, Switzerland, June 14–17, 2010.

[30] Liu, B., Chien, K. and Wang, C., 2004, "Effect of Working fluids on Organic Rankine Cycle for Waste Heat Recovery," Energy, **29**, pp. 1207–1217.

[31] Saleh, B., Koglbauer, G., Wendland, M. and Fischer, J., 2007, "Working Fluids for Low Temperature Organic Rankine Cycle," Energy, **32**, pp. 1210–1221.

[32] Tchanche, B.F., Papadakis, G., Lambrinos, G. and Frangoudakis, A., 2009, "Fluid Selection for a Low Temperature Solar Organic Rankine Cycle," Applied Thermal Engineering, **29**, pp. 2468–76.

[33] Wang, X.D. and Zhao, L., 2009, "Analysis of Zeotropic Mixtures used in Low- Temperature Solar Rankine Cycles for Power Generation," Solar Energy, **83**, pp. 605-613.

[34] Lakew, A.A. and Bolland, O., 2010, "Working Fluids for Low-Temperature Heat Source," Applied Thermal Engineering, **30**, pp. 1262-1268.

[35] Papadopoulos, A.I., Stijepovic, M. and Linke, P., 2010, "On the Systematic Design and Selection of Optimal Working fluids for Organic Rankine Cycles," Applied Thermal Engineering, **30**, pp. 760–769.

[36] Shaaban, S.2016. Analysis of an integrated solar combined cycle with steam and organic Rankine cycles as bottoming cycles. Energy Conversion and Management. 126:1003-12.

[37] Guo, C., Du, X., Goswami, D. Y., Yang, L. Investigation on working fluids selection for organic rankine cycles with low-temperature heat sources, International Journal of Green Energy 13 (2016) 556–565.

[38] Fu, B-R., Lee, Y-R., Hsieh, J-C. Experimental investigation of a 250-kW turbine organic Rankine cycle system for low-grade waste heat recovery, International Journal of Green Energy 13 (2016) 1442-1450.

[39] Yiping Dai, Dongshuai Hu, Yi Wu, Yike Gao, Yue Cao. 2017. Comparison of a Basic Organic Rankine Cycle and a Parallel Double-Evaporator Organic Rankine Cycle. Heat Transfer Engineering. 38: 990-99. doi:10.1080/01457632.2016.1216938.

[40] Wang, E., Yu, Z., Zhang, H., Yang, F. A regenerative supercritical-subcritical dualloop organic Rankine cycle system for energy recovery from the waste heat of internal combustion engines, Applied Energy 190 (2017) 574-590.

[41] Singh, H. and R.S. Mishra. Performance Evaluation of the Supercritical Organic Rankine Cycle (SORC) Integrated with Large Scale Solar Parabolic Trough Collector (SPTC) System: An Exergy Energy Analysis.Environmental Progress & Sustainable Energydoi:10.1002/ep.12735.

[42] Hoang, A.T. 2018. Waste heat recovery from diesel engines based on Organic Rankine Cycle. Applied Energy. 231:138-66.

[43] Li, J., Z. Ge, Y. Duan, Z. Yang, and Q. Liu. Parametric optimization and thermodynamic performance comparison of single-pressure and dual-pressure evaporation organic Rankine cycles. Applied Energy. 217:409–21.

[44] Bellos, E., Tzivanidis, C., Torosian, K. Energetic, exergetic and financial evaluation of a solar driven trigeneration system, Thermal Science and Engineering Progress 7 (2018) 99– 106.

[45] Bellos, E., Tzivanidis, C. Investigation of a hybrid ORC driven by waste heat and solar energy, Energy Conversion and Management 156 (2018) 427–439.

[46] Song, X., X. Chen, L. Qi and Y. Liu.2020.Analysis of a supercritical organic Rankine cycle for low grade waste heat recovery. Proceeding of the Institution of Civil Engineering- Energy 173 (1):3-12.

[47] Moloney, F., E. Almatrafi and D. Y. Goswami. 2020. Working fluid parametric analysis for recuperative super critical organic Rankine cycle for medium geothermal reservoir temperatures. Renewable Energy 147:2874-2881.

[48] Sadoon , S.,and S.M.S. Islam. 2020. Performance analysis of supercritical organic Rankine cycle system with different heat exchanger design configuration. Journal of Advance Research in Fluid Mechanics and Thermal Sciences 65 (2):324-333.261.

[49] Moles, F., J, Navarro-Esbrí , B. Peris , A. Mota-Babiloni, and K. Kontomaris.2015 Thermodynamic analysis of a combined organic Rankine cycle and vapor compression cycle system activated with low temperature heat sources using low GWP fluids, Applied Thermal Engineering 87: 444-453.

[50] Wu, C., S.S. Wang, X.J. Feng, and J. Li.2017. Energy, exergy and exergo-economic analyses of a combined supercritical CO2 recompression Brayton/absorption refrigeration cycle, Energy Conversion Management. 148:360–377.

[51] Saleh, B. 2018. Energy and exergy analysis of an integrated organic Rankine cyclevapor compression refrigeration system. Applied Thermal Engineering 141: 697-710.

[52] H. Li, W. Su, L. Cao, F. Chang, W. Xia, Y. Dai. 2018. Preliminary conceptual design and thermodynamic comparative study on vapor absorption refrigeration cycles integrated with a supercritical CO_2 power cycle, Energy Conversion. Management. 161:162–171.

[53] Pektezel, O. and H.I. Acar. 2019. Energy and exergy analysis of combined organic Rankine cycle- single and dual evaporator vapor compression refrigeration cycle. Applied Science 9:5028. doi:10.3390/app9235028.

[54] Javanshir, N., S. M. S. Mahmoudi, and M. A. Rosen. 2019. thermodynamic and exergoeconomic analyses of a novel combined cycle comprised of vapor-compression refrigeration and organic Rankine cycles. Sustainability 11:3374.

[55] Wang, X., and Y. Dai. 2016. Exergoeconomic analysis of utilizing the transcritical CO2 cycle and the ORC for a recompression supercritical CO2 cycle waste heat recovery: a comparative study, Applied Energy 170:193–207.

[56] Khaliq, A., Kumar, R., Dincer, I. Exergy analysis of an industrial waste heat recovery based cogeneration cycle for combined production of power and refrigeration, Journal of Energy Resources Technology 131 (2009) 022402-1-9.

[57] Wang, X., Dai, Y. Exergoeconomic analysis of utilizing the transcritical CO2 cycle and the ORC for a recompression supercritical CO2 cycle waste heat recovery: A comparative study, Applied Energy 170 (2016) 193-207.

[58] Njoku, I. H., Oko, C.O.C., Ofodu, J. C. Performance evaluation of a combined cycle power plant integrated with organic Rankine cycle and absorption refrigeration system, Cogent Engineering 5 (2018) 1451426-1-30.

[59] Singh, H., and R.S. Mishra. 2018. Performance analysis of solar parabolic trough collectors driven combined supercritical CO2 and organic Rankine cycle. Engineering Science and Technology, an

International Journal 21:451–464.
[60] Keenan, H., Neumann, E.P. and Lustwerk, F., 1950, "An Investigation of Ejector Design by Analysis and Experiment," ASME Journal of Applied Mechanics, **72**, pp. 299–309.
[61] Huang, B.J., Chang, J.M., Wang, C.P. and Petrenko, V.A., 1999, "A 1-D Analysis of Ejector Performance," International Journal of Refrigeration, 22(5), pp. 354–364.
[62] Ouzzane, M. and Aidoun, Z., 2003, "Model Development and Numerical Procedure for Detailed Ejector Analysis and Design," Applied Thermal Engineering, **23**, pp. 2337–2351.
[63] Khaliq, A. and Kumar, R., 2007, "Exergetic Analysis of Solar Powered Absorption Refrigeration System Using LiBr-H2O and NH3-H2O as Working Fluids," International Journal of Exergy, 4(1), pp. 1-18.
[64] Modi, B., Mudgal, A. and Patel, B., 2017, "Energy and Exergy Investigation of Small Capacity Single Effect Lithium Bromide Absorption Refrigeration System," Energy Procedia, 109, pp. 203- 210.
[65] Wang, J., Zhao, P. and Dai, Y., 2016, "Thermodynamic Analysis of a New Combined Cooling and Power System Using Ammonia–Water mixture," Energy Conversion and Management, 117, pp. 335-342.
[66] Rashidi, M.M., Beg, O.A. and Aghagoli, A., 2012, "Utilization of Waste Heat in Combined Power and Ejector Refrigeration for a Solar Energy Source," International Journal of Appl. Math and Mech., 8(17), pp.1-16.
[67] Habibzadeh, A., Rashidi M. M., and Galanis, N., 2013, "Analysis of a Combined Power and Ejector- Refrigeration Cycle using Low Temperature Heat," Energy Conversion and Management, 65, pp. 381-391.
[68] Wang, J., Dai, Y. and Sun, Z., 2009, "A Theoretical Study on a Novel Combined Power and Ejector Refrigeration Cycle," International Journal of Refrigeration, 32, pp. 1186-1194.
[69] Dai, Y., Wang, J. and Gao, L., 2009, "Exergy Analysis, Parametric Analysis and Optimization for a Novel Combined Power and Ejector Refrigeration Cycle," Applied Thermal Engineering, 29, pp. 1983-1990.
[70] Agrawal, B.K. and Karimi, M.N., 2013, "Parametric, Exergy and Energy Analysis of Low Grade Energy and Ejector Refrigeration Cycle," International Journal of Sustainable Building Technology and Urban Development, 4(2), pp. 170-176.
[71] Khaliq A., 2017, "Energetic and Exergetic Performance Investigation of a Solar Based Integrated System for Cogeneration of Power and Cooling," Applied thermal Engineering, 112, PP. 1305-1316.
[72] Khaliq A., Agrawal, B.K. and Kumar, R., 2012, "First and second law investigation of waste heat based combined power and ejector-absorption refrigeration cycle," International Journal of Refrigeration, 35(1), pp. 88-97.
[73] Wang M, Wang J, Zhao P, et al. Multi-objective optimization of a combined cooling, heating and power system driven by solar energy. Energy Convers Manag 2015; 89: 289–297.
[74] Yang X, Zheng N, Zhao L, et al. Analysis of a novel combined power and ejector refrigeration cycle. Energy Convers Manage 2016; 108:266–74.
[75] Zare V and Hasanzadeh M. Energy and exergy analysis of a closed Brayton cycle-based combined cycle for solar power tower plants. *Energy Conversion and Management* 2016; 128:227–237.
[76] Mohtaram. S, Chen. W, Lin. J, Investigation on the combined Rankine absorption power and refrigeration cycles using the parametric analysis and genetic algorithm. Energy Conversion and Management 2017; 150: 754-762.
[77] Patel B, Desai NB, Kachhwaha SS. Optimization of waste heat based organic Rankine cycle powered cascaded vapor compression-absorption refrigeration system. *Energy Conversion and Management* 2017; 54: 576–590.
[78] Saini P, Singh J and Sarkar J. Proposal and performance comparison of various solar-driven novel combined cooling, heating and power system topologies. Energy Convers Manag 2020; 205: 112342.
[79] Dabwan YN and Pei G. A novel integrated solar gas turbine trigeneration system for production of power, heat, and cooling: thermodynamic-economic-environmental analysis. Renew Energy 2020; 152: 925–941.
[80] Khan Y and Shyam Mishra R. Thermo-economic analysis of the combined solar based pre- compression supercritical CO_2 cycle and organic Rankine cycle using ultra low GWP fluids. Therm Sci Eng Prog 2021; 23: 100925.
[81] Khan Y and Mishra RS. Performance evaluation of solar based combined pre-compression supercritical CO_2 cycle and organic Rankine cycle. Int J Green Energy 2021; 18(2): 172–186.
[82] Mahdavi N, Ghaebi H and Minaei A. Proposal and multi-aspect assessment of a novel solar-based trigeneration system; investigation of zeotropic mixture's utilization. Appl Therm Eng 2022; 206: 118110.
[83] Ahmadi A, Ehyaei MA, Doustgani A, et al. Recent progress in thermal and optical enhancement of low temperature solar collector. Energy Syst 2023; 14: 1–40.
[84] Khan Y, Caliskan H and Hong H. A comparative study of combined cycles for concentrated solar power for efficient power generation using low global warming potential (GWP) fluids to reduce environmental effects. IET Renew Power Gener 2023; 17: 3741–3754.
[85] Alharthi MA, Khaliq A, Alqaed S, et al. Investigation of new combined cooling, heating and power system based on solar thermal power and single-double-effect refrigeration cycle. Energy Rep 2023; 9: 289–309.
[86] Khan Y, Singh D, Caliskan H, et al. Exergoeconomic and thermodynamic analyses of solar power tower based novel combined helium Brayton cycletranscritical CO_2 cycle for carbon free power generation. Glob Chall 2023; 7: 2300191.
[87] Faruque MW, Khan Y, Nabil MH, et al. Parametric analysis and optimization of a novel cascade compression-absorption refrigeration system integrated with a flash tank and a reheater. Results Eng 2023; 17: Article no. 101008.
[88] Askari IB, Ghazizade-Ahsaee H and Kasaeian A. Investigation of an ejector-cascaded vapor compression–absorption refrigeration cycle powered by linear Fresnel and organic Rankine cycle. Environ Dev Sustain 2023; 25: 9439–9484.
[89] Zhou J, Ali MA, Zeki FM, et al. Thermoeconomic investigation and multi-objective optimization of a novel efficient solar tower power plant based on supercritical Brayton cycle with inlet cooling. Therm Sci Eng Prog 2023; 39: 101679.

Cite this article as: Radhey Shyam Mishra, Aftab Anjum, Energy-exergy analysis of solar assisted some trigeneration Systems International Journal of Research in Engineering and Innovation Vol-9, Issue-3 (2025), 72-95.
https://doi.org/10.36037/IJREI.2025.9301